The Caraguataí syenitic suite, a ca. 2.7 Ga-old alkaline magmatism (petrology, geochemistry and U–Pb zircon ages). Southern Gavião block (São Francisco Craton), Brazil

Simone Cerqueira Pereira Cruz [a,*], Jean-Jacques Peucat [b], Leo Teixeira [c], Maurício Antônio Carneiro [d], Adriano Alberto Marques Martins [d], Jocilene dos Santos Santana [d], Jailma Santos de Souza [a], Johildo Salomão Figueiredo Barbosa [a], Ângela Beatriz Menezes Leal [a], Elton Dantas [e], Marcio Pimentel [e]

[a] Universidade Federal da Bahia (UFBA), Departamento de Geologia e Geofísica Aplicada, Centro de Pesquisa em Geofísica e Geologia, Rua Barão de Geremoabo, s/n, Federação, 40170 209 Salvador, Bahia, Brazil
[b] Géosciences Rennes, UMR CNRS 6118, Université de Rennes-1, 35042 Rennes Cedex, France
[c] Geological Survey of Brazil (CPRM), Av. Ulysses Guimarães, 2862, Sussuarana, Centro Administrativo da Bahia, Salvador 41213 000, Bahia, Brazil
[d] Universidade Federal de Ouro Preto (UFOP), Departamento de Geologia, Morro do Cruzeiro, Ouro Preto-Minas Gerais, CEP: 30.400 000, Brazil
[e] Universidade de Brasília (UnB), Instituto de Geociências, Campus Universitário Darcy Ribeiro CEP 70910-900 Brasília, DF, Brazil

ARTICLE INFO

ABSTRACT

The Gavião Block comprises amphibolite- and granulite-facies gneisses and migmatites of tonalitic, granodioritic and granitic compositions and supracrustal sequences including volcanosedimentary layers metamorphosed up to the amphibolite facies. In the region of Abaíra-Jussiape (BA), two main igneous suites, called Caraguataí and Jussiape, are exposed in the core of an anticline. The Caraguataí suite encompasses alkali-feldspar granites, syenites and quartz syenites that contain biotite, magnetite/ hematite, apatite, titanite, hastingsite/pargasite and zircon as accessory minerals that were adjusted to the amphibolite facies. White mica and epidote minerals are related to retrograde greenschist facies. These rocks were deformed in dextral to reverse-dextral shear zones, giving origin to protomylonites and augen-mesomylonites to ultramylonites. The ultramylonites have a prominent banding parallel to the main foliation of the rocks. Lithogeochemical studies revealed subalkaline to alkaline, metaluminous to peraluminous, Fe-rich protolith for instead of to these rocks associated with A2-type magmatism and partial melting of igneous continental crust. In situ U–Pb zircon dating using the Laser Ablation ICPMS method was carried out for five samples of the Caraguataí alkaline suite. The ages obtained for an isotropic syenite (SCP 1470: 2680 ± 24 Ma), a foliated syenite (SCP 2035: 2703 ± 11 Ma), a syenitic augen gneiss (SCP 2017: 2706 ± 34 Ma) and two ultramylonitic syenitic banded gneisses (SCP 1446: 2711 ± 34 Ma and SCP 1809: 2698 ± 10 Ma) fall in the same range. The average of the 62 concordant analyses obtained from the five samples allows to determine a mean $^{207}Pb/^{206}Pb$ age of 2696 ± 5 Ma ($\pm 2\sigma$) interpreted as that of the alkaline plutonism. The geochronologic data obtained up to now have not helped to constrain an age for the metamorphism that affected the study area. The A2 type of magmatism, instead of and the T_{DM} model ages (ca. 3.2–3.8 Ga) and the corresponding negative $\varepsilon(t)$ values (-4 to -6), suggest that the alkaline magmas are mainly derived from partial melting of Paleo-archean gneisses in an intraplate setting similar to those from the surrounding Aracatu region. The isotopic data obtained in this work together with published data suggest that in the southern sector of the Gavião Block an important event of crustal recycling occurred ca. 2.7 Ga ago. Similar ages have been found in other parts of the São Francisco Craton.

* Corresponding author. Tel.: +55 71 55 3012 7028.
E-mail addresses: simoneufba@gmail.com (S.C.P. Cruz), peucat@univ-rennes1.fr (J.-J. Peucat), leo.teixeira@cprm.gov.br (L. Teixeira), mauricio@degeo.ufop.br (M.A. Carneiro), adriano1952@gmail.com (A.A. Marques Martins), jocilenesanttana@ yahoo.com.br (J.dosS. Santana), johildo@cpgg.ufba.br (J.S.F. Barbosa), angelab@ ufba.br (Â.B.M. Leal), elton@unb.br (E. Dantas), marcio@unb.br (M. Pimentel).

1. Introduction

The northern part of the São Francisco Craton can be divided in four main tectonic units: the Gavião, Jequié, Itabuna-Salvador-Curaçá and Serrinha blocks, all formed of instead of by Archean and Paleoproterozoic terrains (references in Table 1). These blocks can

Table 1
Main geochronological data for the rocks from the Gavião Block and neighboring units. Modified after Bastos Leal (1998). 1 – Cordani and Iyer (1979); 2 – Marinho et al. (1979); 3 – Cordani et al. (1985); 4 – Turpin et al. (1988); 5 – Wilson et al. (1988); 6 – Mascarenhas and Garcia (1989); 7 – Sabaté et al. (1990); 8 – Marinho (1991); 9 – Martin et al. (1991); 10 – Cordani et al. (1992); 11 – Ledru et al. (1993); 12 – Nutman and Cordani (1993); 13 – Nutman et al. (1993); 14 – Pimentel et al. (1994); 15 – Rosa et al. (1996); 16 – Barbosa and Dominguez (1996); 17 – Bastos Leal et al. (1997); 18 – Cordani et al. (1997); 19 – Martin et al. (1997); 20 – Santos-Pinto et al. (1998); 21 – Bastos Leal et al. (1998); 22 – Sato (1998), 23 – Bastos Leal (1998); 24 – Bastos Leal et al. (2000); 25 – Lopes (2002); 26 – Bastos Leal et al. (2003); 27 – Guimarães et al. (2005); 28 – Marinho et al. (2008).

Unidades geológicas	U–Pb (zircon) and ^{207}Pb/^{206}Pb (Ma)	Rb–Sr (WR) (Ga)	^{207}Pb/^{206}Pb (Ga)	Sm–Nd (T_{DM}) (Ga)	K–Ar (Ga)	References
Sete Voltas granitoid	3403, 3243 ± 5, 3158 ± 2	3.4; 3.2; 3.1, 2.6	3.2	3.7–3.5	1.9–1.8	3, 6, 9, 12, 19
Boa Vista/Mata Verde gneiss	3.353 ± 5	3.3	3.4	3.5–3.2	0.9–0.4	3, 5, 6, 8, 12
Bernarda tonalite	3332 ± 4	2.6–2.7		3.3–3.5		3, 20
Mariana and Aracatu granitoids	3245 ± 25, 3250 ± 4, 3240 ± 14 Ma, 3.325 ± 10, 2506 ± 10, 1944 ± 7	0.5		3.6–3.5	0.6–0.5	20
Piripá gnaisses	3200 ± 5	2.7 and 2.0		3.5–2.9	0.6	6, 18, 22
Lagoa do Morro granitoid	3184 ± 6	3.2 and 2.8	2.8	3.6–3.3	0.6–0.5	2, 3, 7, 8, 9
Serra do Eixo granite	3158 ± 5, 2.5–2.6, 2695 ± 5			3.3		20
Serra dos Pombos granite	2845 ± 45	2.8	2.8			8, 12
Gneissic and migmatitic rocks	3200 ± 11	2.7 and 1.9–1.8		3.4–3.1	0.6–0.5	6, 17, 22
Malhada de Pedra granite		2.8		3.27		17, 21
Lagoa da Macambira granite	3146 ± 24	2.84	3.1–3.2	3.34		21, 23
Serra do Eixo Alkaline Granites	2500–2600			3.3		17, 20
Rio Jacaré Sill		1.9	2.5	3.5–3.3		6, 8
Pé de Serra SubAlkaline and Alkaline Granites	2652 ± 1, 2282 ± 81	2.6–2.2, 1.2	2.6; 2.3	3.2–3.1	2.0–1.8	3, 8, 28
Umburanas granite	2049 ± 5			3.3		20
Serra da Franga granite	2039 ± 11					20
Mariana granite	3259 ± 5 Ma, 1944 ± 7			3.5–3.6		20
Aracatu granite	3240 ± 1, 3.371 ± 14, 3325 ± 10, 2506 ± 10, 2149 ± 15, 1.95–2.26			3.6		7, 8, 20
Gameleira granite		1.95		2.6–2.8		7, 8
Riacho Pedras granite		1.9		3.2		7, 8
Lagoa Grande/Lagoinha granites		2.0		2.7–2.9		7, 8
Iguatemi granite		2.03		2.9–3.5	0.48	24
Rio do Paulo granite		1.96		2.73	0.50	24
Espírito Santo granite	2.01, 2023 ± 26, 997 ± 32	1.6		3.05–3.09	0.49	24
Caculé granite	2.02, 2070 ± 72, 1956 ± 56, 2070 ± 72	1.9		2.63–2.77	1.06–0.55	20, 24
Guajeru TTG Terrane	3191–3394					25
Jussiape granite	2122					27
Veredinha granitoid	2103					27
Ibitiara granitoid	2091					27
Guajeru Alkaline Granite	2649–2660					25
Contendas Mirante – Upper Unit	2150–1900					3, 8
Contendas Mirante – Intermediate Unit		2.2 and 1.2	2.5	3.4–3.2		3, 8
Contendas Mirante – Lower Unit		2.5 and 2.0		3.3–3.0	2.0–1.5	3, 8
Umburanas – Intermediate Unit		2.2	2.7 and 2.0		1.0-05	3, 26
Lagoa Real Complex – Gneissic Rocks		2.7				4, 10, 14
Lagoa Real Complex – São Timóteo Granite	1746 ± 5	1.7	1.7	2.7–2.9	0.5	4, 10, 14, 22
Lagoa Real Complex – Albitites	1745 ± 15; 961 ± 22	1.5				4, 10, 14

also be characterized by Nd isotopes which indicate the dominant crust involved. Indeed, each bock corresponds to specific ranges of Nd model ages (Barbosa and Sabaté, 2002), which are 2.9–3.6 Ga, 2.7–3.0 Ga, 2.4–2.6 Ga and 3.0–3.2 Ga in the Gavião, Jequié, Ita-buna-Salvador-Curaçá and Serrinha blocks, respectively (Fig. 1). The set of available geochronological data for the Gavião Block (Fig. 2) reveals a polycyclic evolution that marks three main periods of magmatism with ages ranging between 3.4–3.2 Ga, 3.2–3.1 Ga and 2.9–2.7 Ga (Santos-Pinto et al., 1998, submitted for publication; Bastos Leal et al., 1998). Despite being recognized by some authors, the Neoarchean evolution of the Gavião block is still poorly studied. In its southern part, close to Jussiape, the Caraguataí pluton crops out as a Neoarchean alkaline suite (this work, Figs. 2 and 3). It occurs as a structural window in instead of into the Gavião gneissic Archean basement and its exposure is related to the uplifted Abaíra-Jussiape core, affecting the Proterozoic cover. This paper presents petrological and geochemical results, Nd isotope data and U–Pb zircon ages obtained for the Caraguataí syenitic suite (originally named Caraguataí Complex by Lopes, 1991). The aim of this work is to present the results of the petrologic, geochemical and geochronologic studies of Neoarchean rocks that crop out in the southern portion of the Gavião Block.

2. Geological setting of the Gavião block

In the Gavião Block (Fig. 2) various gray orthogneisses, granit-oids and supracrustal sequences of Archean and Paleoproterozoic ages can be recognized (see references in Table 1). Previous geochronological data have shown that the formation of the Gavião Block is related to at least three Archean events. The first one is Paleoarchean and took place around 3.4–3.2 Ga (Martin et al., 1991; Nutman and Cordani, 1993; Cunha et al., 1996; Santos-Pinto, 1996; Santos-Pinto et al., 1998, submitted for publication; Bastos Leal et al., 1996, 1998; Bastos Leal, 1998; Peucat et al., 2002), and corresponds to several inputs of tonalitic–granitic and
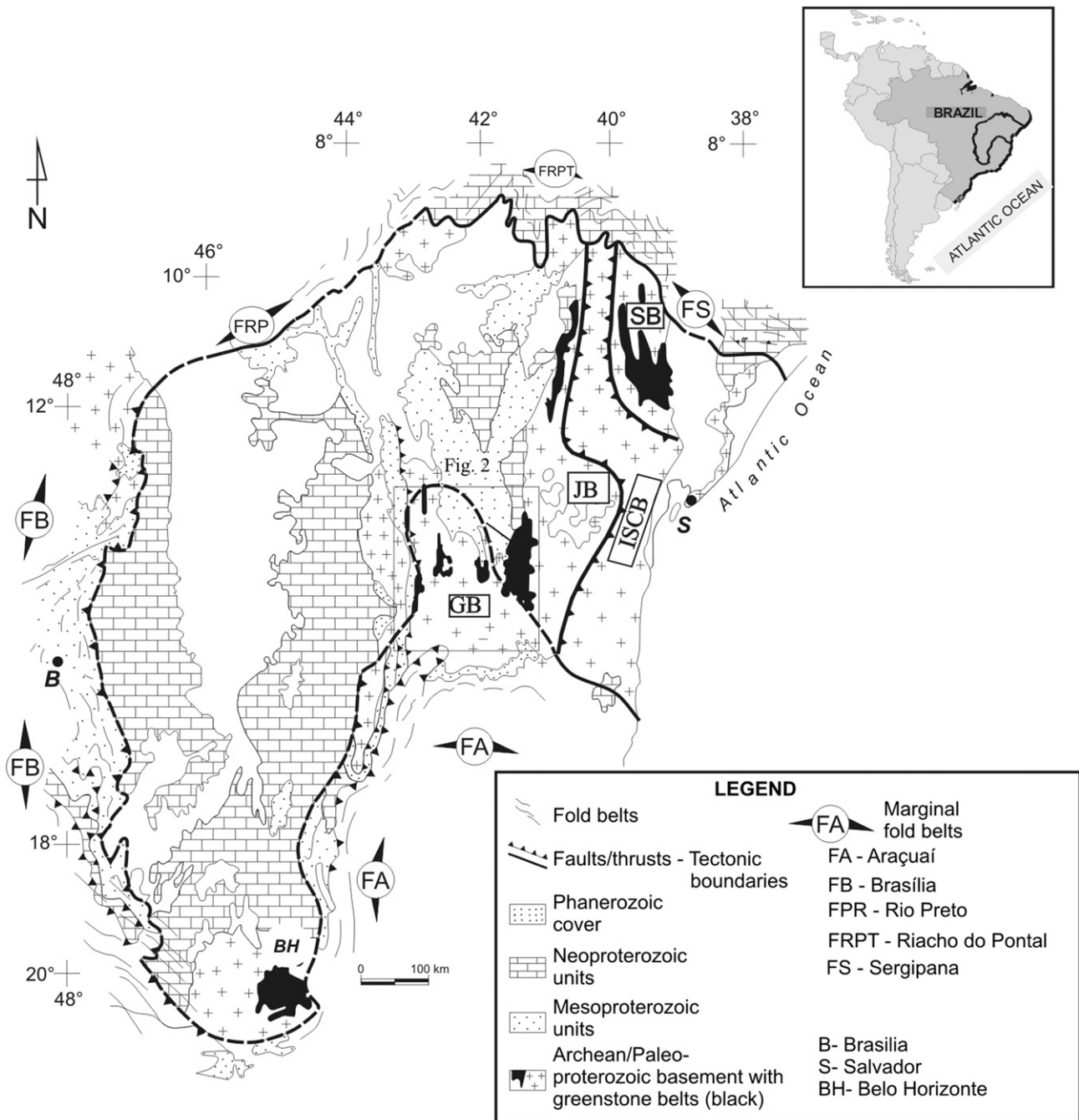
Fig. 1. Schematic geological map showing the limits, marginal fold belts and major structural units of the São Francisco Craton. GB – Gavião Block, JB – Jequié Block, SB – Serrinha Block, ISCB, Itabuna-Salvador-Curaçá Block (adapted from Alkmin et al., 1993). The gray rectangle indicates the study area.

trondhjemitic suites. Such magmas generated from a 3.5 to 3.8 Ga old primitive crust (Santos-Pinto et al., submitted for publication).

Zircon ages presented by Marinho (1991), Martin et al. (1991), Nutman and Cordani (1993), Santos-Pinto (1996), Santos-Pinto et al. (1998), Bastos Leal et al. (1997, 1998), Bastos Leal (1998) and Barbosa et al. (2001) indicate the occurrence of a second Meso-archean plutonic event with ages between 3.2 and 3.1 Ga (Table 1). This event, which produced partial melting of the previous crust is represented by a set of plutonic suites of granitic and granodioritic compositions (Santos-Pinto, 1996; Santos-Pinto et al., 1998; Bastos Leal et al., 1997; Bastos Leal, 1998). Crustal reworking process is also

shown by Nd T_{DM} model ages which are all higher than 3.0 Ga and by negative epsilon Nd (t) values (Martin et al., 1991, 1997; Bastos Leal, 1998).

The third Archean plutonic event was indicated by whole-rock Rb–Sr and zircon evaporation TIMS data that yielded ages between 2.9 and 2.7 Ga (Brito-Neves et al., 1980; Costa et al., 1985; Cordani et al., 1985; Nutman and Cordani, 1993; Santos-Pinto et al., 1998). Jardim de Sá (1981) obtained a Rb–Sr age of 2600 ± 80 Ma for the Paramirim gneisses. A SHRIMP zircon age of 2693 ± 5 Ma is defined for the magmatic alkaline suite recognized in the Serra de Eixo gneisses (Santos-Pinto et al., submitted for publication).
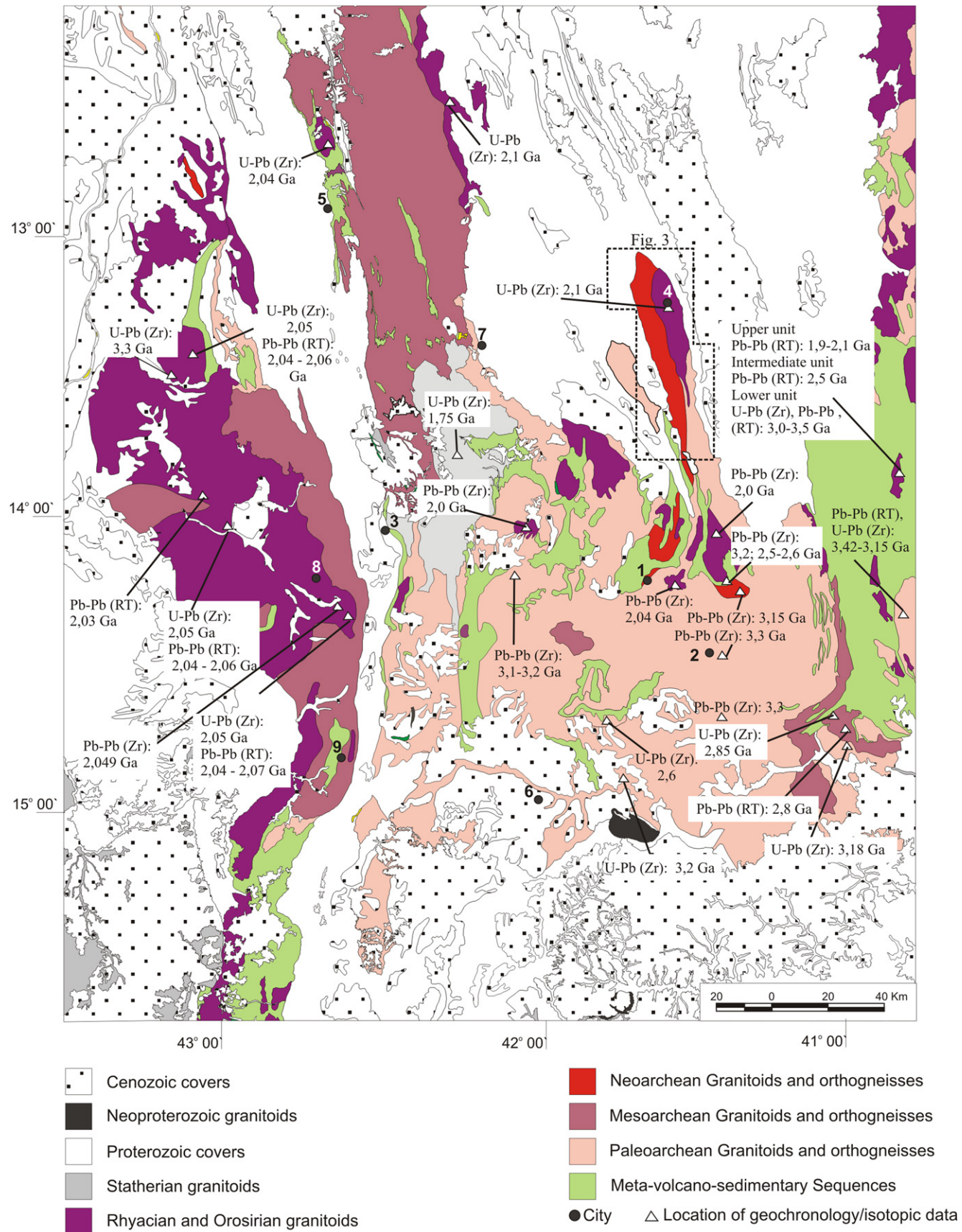
Fig. 2. Simplified geologic map encompassing the Gavião Block, Paleoproterozoic Lagoa Real Complex granitoids, and Proterozoic Espinhaço and São Francisco Supergroup covers. The rectangle represents the area of the Abaíra-Jussiape Anticlinal. Cities: 1 — Brumado, 2 — Aracatu, 3 — Caetité, 4 — Jussiape, 5 — Macaúbas, 6 — Condeúba, 7 — Paramirim, 8 — Guanambi, 9 — Urandi.
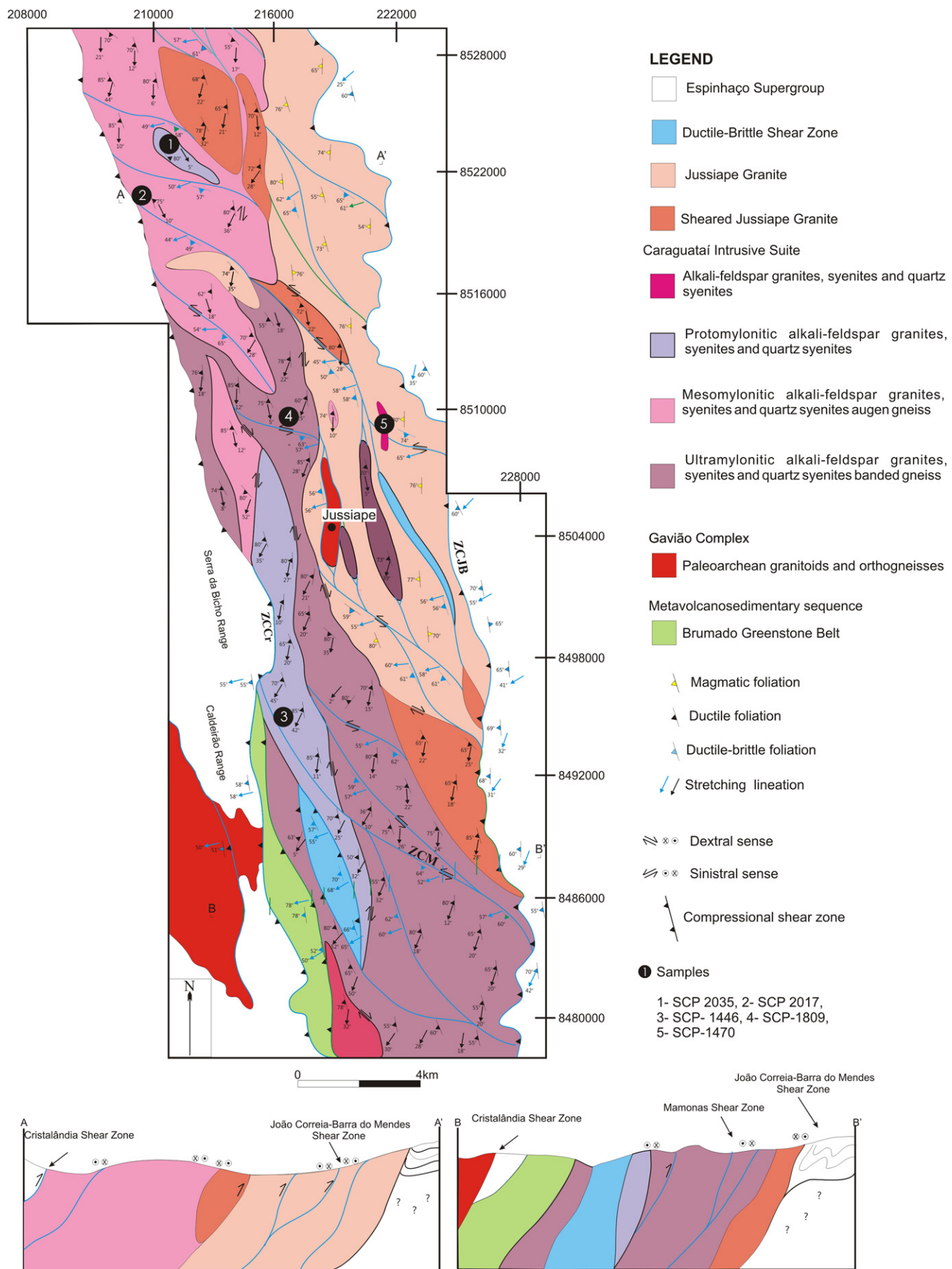
Fig. 3. Geologic map of the Abaíra-Jussiape Anticlinal Nucleus. ZCJB – João Correia-Barra do Mendes Shear Zone, ZCM – Mamonas Shear Zone, ZCCr – Cristalândia Shear Zone.

Marinho et al. (2008) obtained a SHRIMP zircon age of 2652 ± 11 Ma for the alkaline gneisses of Pé de Serra. Costa et al. (1985) and Cordani et al. (1992) obtained Rb–Sr ages for the host rocks of the Lagoa Real paleoproterozoic intrusive suite ranging between 2.9 and 2.7 Ga. Bastos Leal et al. (1998) obtained a zircon TIMS evaporation age of 2.75 Ga for a felsic volcanic of the Umburanas greenstone belt.

The metasedimentary rocks of Paleoproterozoic and Archean ages (Fig. 2) can be grouped in the Contendas Mirante, Mundo Novo, Ibitira-Ubiraçaba, Brumado, Guajeru and Riacho de Santana greenstone belts, in the Urandi and Boquira metavolcanosedimentary sequences and in the Licinio de Almeida metasedimentary sequence (Silva and Cunha, 1999).

The Lagoa Real Complex (Fig. 2) is a meta-syenite-alkali feldspar granitic suite of Statherian age, ca. 1.7 Ga old (Turpin et al., 1988; Pimentel et al., 1994; Cordani et al., 1992; Cruz et al., 2007). It was previously called São Timóteo granite by Fernandes et al. (1982) or Lagoa Real granite by Cruz et al. (2007). It is associated with orthogneisses, albitites, oligoclasites, microclinites, amphibolites and meta-gabbronorites (Costa et al., 1985; Lobato, 1985; Lobato and Fyfe, 1990; Arcanjo et al., 2000; Cruz, 2004). These are continental intraplate granitoids related to the opening of the Paramirim Aulacogen (Teixeira, 2000).

The Proterozoic covers comprise the Espinhaço and São Francisco supergroups (Fig. 2). The Espinhaço Supergroup comprises a succession of essentially terrigenous sedimentary rocks, with contributions of underlying intermediate to felsic volcanics, deposited from 1.7 Ga (Schobbenhaus et al., 1994; Babinski et al., 1999; Danderfer Filho, 2000; Danderfer Filho and Dardenne, 2002) until 1.0 Ga. Several stratigraphic columns were proposed for this supergroup in Bahia State (Schobbenhaus, 1996; Barbosa and Dominguez, 1996; Danderfer Filho, 2000; Guimarães et al., 2005; Loureiro et al., 2010). The volcanic units of the Espinhaço Supergroup chronocorrelate with the Lagoa Real suite and should reflect the volcanism related to the opening of the Paramirim Aulacogen (McReath and Sabaté, 1987; Arcanjo et al., 2000).

Gabbroic rocks frequently occur in the Espinhaço Supergroup as intrusive discontinuous sills and dikes. Laser ablation (U–Pb) zircon dating revealed two age groups: Group I: 1492 ± 16 Ma (Loureiro et al., 2010); 1514 Ma (Babinski et al., 1999) and 1496 Ma (Guimarães et al., 2005); Group II: 854 ± 23 Ma (Danderfer Filho et al., 2009) and 834 Ma (Loureiro et al., 2010).

The São Francisco Supergroup comprises terrigenous and carbonate rocks deposited by marine-influenced glaciogenic processes (Guimarães, 1996) and the maximum age is 800 Ma (Misi and Veizer, 1996).

The Caraguataí suite, object of this work, is located ca. 50 km northeast of Brumado (Fig. 2). Its southern part is emplaced into Archean gray gneisses similar to those described in the Aracatu region (Santos-Pinto et al., 1998, submitted for publication) and into the Brumado greenstone belt. It is intruded by the Paleoproterozoic Jussiape granite (Fig. 3) and is in tectonic contact with the Espinhaço sedimentary sequence through low-temperature, reverse-dextral shear zones of Neoproterozoic age. This suite also occurs in the basement of the Western Chapada Diamantina Thrust-Fold Belt (Danderfer Filho, 1990, 2000; Cruz et al., 2007), in the northern Araçuaí Orogen (Pedrosa-Soares et al., 2007).

3. Petrography of the Caraguataí suite

The Caraguataí suite (Fig. 3) consists of alkali-feldspar granites, syenites and quartz syenites. The rocks are leuco- to mesocratic with pale gray color. The igneous protolith is progressively deformed in NNW–SSE dextral to dextral-reverse shear zones, giving rise to protomylonites, augen-mesomylonites to ultramylonites (Fig. 4a–c), reaching amphibolite facies conditions. These tectonites are truncated by thin reverse to reverse-dextral shear zones trending NNW–SSE that host greenschist facies phyllonites and that were responsible for the uplift of the Abaíra-Jussiape basement core.

The protomylonites (Fig. 4a) exhibit porphyroclasts generally ca. 4 cm in size, some reaching 8 cm. Foliation is marked by biotite, and
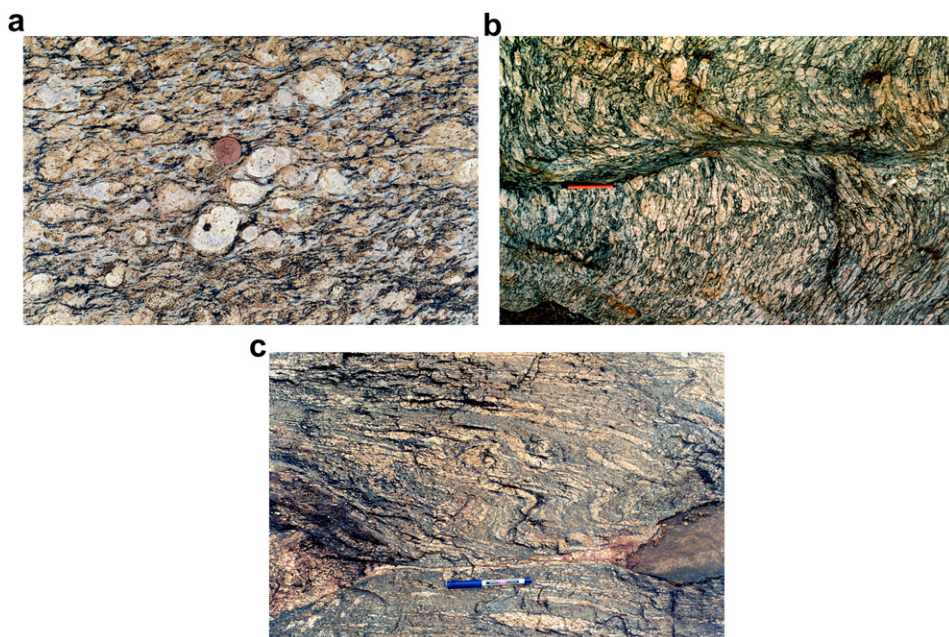

Fig. 4. Caraguataí Suite rocks: (a) protomylonitic, (b) augen-mesomylonitic, and (c) ultramylonitic facies.

in some cases, amphibole is still incipiently developed and discontinuous. Fig. 4b shows zones of greatest strain in the augen-mesomylonites and Fig. 4c shows that the mylonitic foliation is parallel to the gneissic banding. This banding is marked by milli-meter- to centimeter-sized felsic layers, which alternate with mafic layers enriched in amphibole and biotite. The average modal composition is alkali feldspar (70−85%), plagioclase (0−10%), quartz (2−25%), brown biotite (5−12%), magnetite/hematite (2−6%), apatite (1−2%), titanite (1−2%), hastingsite/pargasite (1−2%) and zircon (1−3%), which were adjusted in the amphibolite facies. White mica (1−2%) and epidote (0−2%) are minerals related to retrograde greenschist facies metamorphism. Microstructures observed in thin sections as relicts of the igneous protolith, with equigranular to porphyritic textures and poikilitic inclusions of amphibole in K-feldspar, indicate the igneous origin of these rocks. Deformational processes at the grain scale are associated with intracrystalline plasticity and with mechanisms of recrystallization which were developed by rotation of subgrains of K-feldspar, plagioclase and quartz. This suggests a temperature of deformation above 550 °C (Tullis, 1983; Simpsom, 1985, 1986; Vauchez, 1987; Stipp et al., 2002).

3.1. Geochemistry

A concern when it comes to metamorphosed and polydeformed rocks such as those of the Caraguataí Suite is to know which is the protolith composition and which is the interference of meta-morphism in the composition of the final products. In the present case a direct definition is impossible, because all the crustal segment was affected by high-grade metamorphism and there are no preserved rocks. The means to reach the protoliths is to define the contents of the chemical elements and their characteristics in orthogneisses and compare them with other plutons of similar composition of other regions, which have not undergone meta-morphism. Such procedure has been used for many years to the petrogenetic characterization of orthogneiss protoliths (Waever and Tarney, 1980; Condie and Allen, 1984; Jahn and Zhang, 1984; Martin et al., 1997, 2005, among others). The analytical data for the Caraguataí orthogneisses were compared with those for several worldly known massifs of similar composition, e.g. White Mountain (Eby, 1990), PykesPeak (Smith et al., 1999) and others listed in Whalen et al. (1987). No deviation that could compromise the interpretation and attributed to metamorphism was observed.

Fifty-three whole-rock analyses of major and trace elements were carried out at GEOSOL − Geology and Surveying Ltd. labora-tories for granites, mylonitic gneiss and augen gneiss and are reported in Table 2. Major (SiO_2, Al_2O_3, FeO, Fe_2O_3, MgO, CaO, TiO_2, P_2O_5, MnO) and trace (Rb, Cs, Ba, Sr, Ga, Ta, Nb, Hf, Zr, Y, Th, U, W, Sn, Cl, S) elements were analyzed by X-ray fluorescence, Cr, Ni, Co, V, Pb, Zn, Cu and Mo by atomic absorption, F by ion-specific electrode, and REE by ICP−MS. Na_2O and K_2O were determined by atomic absorption spectrometry.

The majority of the samples (Table 2) exhibit SiO_2 contents higher than 70 wt.% and the total range is between 69 and 77 wt.%. High SiO_2 values suggest that the Caraguataí suite is strongly differentiated. It is also potassic, with K_2O/Na_2O ratios mostly between 1.3 and 2, and metaluminous to peraluminous (ISA = 0.9−1.2), with an agpaitic index [AI = (Na + K)/Al molar] between 0.75 and 0.95. Liégeois et al. (1998) consider 0.87 as the lower AI limit for alkaline rocks. High total Fe_2O_3 contents together with low MgO contents result in Fe/(Fe + Mg) ratios above 0.90. According to this criterion, the Caraguataí pluton is characterized as a subalkaline to alkaline suite. Furthermore, the high Fe/Mg ratios above 0.90 indicate that the Caraguataí suite belongs to the A-type magmatism (Whalen et al., 1987; Frost et al., 2001).

Subalkaline evolution of major elements in A-type alkaline suites is instead of are frequently reported in the literature (e.g. Whalen et al., 1987; Emslie, 1991; Duchesne and Wilmart, 1997). The modified diagram of De La Roche et al. (1980), which has the advantage of presenting the behavior of all major elements at the same time and therefore avoiding the use of several binary diagrams, shows the trends of three petrogenetic lineages. Fig. 5 shows that the samples plot along the final segment of the sub-alkaline trend within a very narrow fractionation interval. In the AFM diagram (Fig. 6) of Irvine and Baragar (1971) the samples plot along a parallel trend to the AF axis because of high alkalis contents and high (Fe/Fe + Mg) values. Some samples plot in the A-type granitoids field of Whalen et al. (1987) (Fig. 5).

These rocks exhibit high contents of incompatible elements (Table 2), especially HFSE such as Y (up to 50 ppm) and Zr (>400 ppm), and high total REE and F contents (>500 ppm). High contents of halogens such as F, associated with high Zr, Nb, Ta, Y and REE and low Eu and Sr contents are important attributes of A-type granitoids (Best, 2003). These characteristics are also shown in the Figs. 7 and 8 diagrams. Spiderdiagrams (Fig. 7) normalized to primitive mantle values (Wood et al., 1979) are marked by the enrichment of LILE (Rb, Th, K), HFSE, particularly Zr, Tb, and Y, and a strong negative Sr anomaly.

The REE spectra (Fig. 8) show enrichment in LREE and flat HREE patterns. The parallelism between the limits of the envelopes indicates similar mineral fractionation process in all rock types for various total REE contents. $(La/Yb)_N$ ratios are low between 7 and 15.

The lack of intermediate SiO_2 values rules out an origin from simple instead of simply fractional crystallization of a mantle liquid. The lack of less differentiated enclaves attests to the idea that they are not purely mantle-derived. The origin of A-type granitoids is very controversial especially when it comes to composition, which can vary a lot from a place to another. The origin of those having compositions similar to the granitoids of this study has been attributed to partial melting of igneous continental crust, from the residue of a previous melting (Collins et al., 1982; Whalen et al., 1987), which is a very contested hypothesis, or from tonalitic/granodioritic terms (Creaser et al., 1991; Patiño Douce, 1997), which is apparently more feasible. However Eby (1990) considers that the A-type granites result from complex processes and that no single model satisfactorily answers to all A-type granite characteristics.

Patiño Douce (1997) emphasized that the composition of the liquids produced by continental crust melting greatly depends on the pressure. This author showed that it is possible to produce liquid with composition similar to potassic, high SiO_2, metal-uminous to slightly peraluminous, A-type granites from partial melting of tonalitic/granodioritic continental crust. Melting prod-ucts of a tonalite at 4 kb have compositions similar to A-type granites; when the pressure is higher (8 kb), the liquid produced tends to be different.

Thus, crustal melting in shallower depths than 15 km can orig-inate A-type granites. At these low pressures plagioclase is stable and retains in the melting residue elements such as Sr and Eu. Other minerals such as garnet, for example, whose partition coef-ficients are very high for HREE, Y and other HFSE, frees such elements to the liquid being produced, which will enrich in these elements. The composition of the liquid that produced the Car-aguataí Suite granitoids was coherent with this reasoning. Figs. 7 and 8 show that a small interval of fractional crystallization may have existed where K-feldspar was a fundamental component, leading to the strong negative Ba and Eu anomalies.

In Fig. 9, the points that represent the Caraguataí orthogneisses plot in the intraplate granitoids field (WPG). Samples with such characteristics can be plotted in Eby's (1992) diagram (Fig. 10),

Table 2
Chemical compositions of the Caraguataí Suite rocks. Oxides in wt.% and trace elements in ppm.

Sample	2016joc	sj25	1446	1977joc	sj08b	2017	sj05	1809e1joc	sj05d	1794	2035a	1458	1447	1713	1830	2014.1joc	1832	1450a	sj02
SiO_2	69.11	69.60	70.60	70.65	70.70	71.10	71.20	71.90	71.90	72.00	72.00	72.10	72.30	72.30	72.50	72.62	72.70	72.80	72.80
TiO_2	0.58	0.71	0.68	0.34	0.10	0.59	0.47	0.53	0.14	0.54	0.33	0.48	0.62	0.55	0.48	0.19	0.62	0.60	0.64
Al_2O_3	13.74	11.80	12.60	11.34	14.80	12.90	12.20	12.07	14.60	12.60	12.50	11.80	12.50	11.90	11.50	13.98	12.40	12.20	12.00
Fe_2O_3	4.98	2.09	1.66	5.98		1.96	0.71	5.03	0.74	0.97	0.59	2.29	2.66	1.43	1.50	2.53	1.50	2.65	1.57
FeO	2.24	4.74	4.37	4.17	1.64	2.89	3.92	2.44	1.86	3.48	2.63	2.20	2.62	3.61	3.49	1.09	3.76	2.64	3.77
MnO	0.06	0.07	0.08	0.03	0.01	0.08	0.07	0.06	0.03	0.06	0.04	0.05	0.04	0.07	0.05	0.02	0.08	0.06	0.05
MgO	0.58	1.92	0.68	2.99	0.20	0.63	0.42	0.43	0.26	0.66	0.28	0.42	0.61	0.47	0.93	0.26	0.55	0.67	0.75
CaO	1.89	1.12	2.48	0.50	0.41	1.96	1.18	1.37	1.13	1.54	1.02	1.13	1.59	1.56	0.31	0.62	2.09	1.88	1.76
Na_2O	3.21	2.10	2.70	1.91	2.40	3.00	2.90	2.84	3.40	2.50	2.70	2.60	3.20	2.70	1.60	3.36	2.70	2.70	2.90
K_2O	4.67	5.30	4.40	4.91	8.50	4.30	4.70	4.74	5.40	5.00	5.60	5.10	4.20	5.10	5.80	5.64	4.80	4.00	3.10
P_2O_5	0.14	0.16	0.16	0.03	0.08	0.14	0.11	0.11	0.03	0.13	0.06	0.10	0.14	0.11	0.10	0.08	0.14	0.13	0.14
LOI	9.00	0.22	0.15	0.90	0.12	0.22	0.17	0.70	0.25	0.26	0.26	0.15	0.04	0.06	0.41	0.50		0.06	0.22
Total	110.20	99.83	100.56	103.75	98.96	99.77	98.05	102.22	99.74	99.74	98.01	98.42	100.52	99.86	98.67	100.89	101.34	100.39	99.70
Cr	*			*				17.8								*			
Ni	17.2			8				19.7								13			
Co	6.9			3.6				6.1								1.8			
V	20	37	28	*		22	18	18		31	13	18	26	21	15	6	24	28	23
Cu	7.1			2.6				6								2.3			
Pb	11.4			6.2				13.8								17.6			
Zn	55			33				57								35			
Rb	183.6	220	156	156.1	283	194	450	160.6	300	251	439	210	155	253	188	278.7	208	176	216
Cs	1.9			3.5				0.5								1.5			
Ba	659.9	1642	842	3004	1511	965	630	1195.6	733	847	769	1167	1070	1210	1928	312	1050	1160	1617
Sr	73.9		32	39.4	23	12		67.9	34					17		42.5	14	20	41
Ga	25.8	14	16	20.1	17	18	19	22.6	21	19	20	20	18	17	16	22.5	17	18	20
Ta	5.5			3				2								5.1			
Nb	81.7	65	50	44.5	12	59	68	42.3	22	64	43	64	63	82	54	49.1	53	67	67
Hf	15.7			17				0.5								7			
Zr	287.6	646	444	632		560	530	683.8	206	421	352	553	560	625	508	203.1	567	571	741
Y	176.8	175	93	102.3	58	127	372	116.7	71	322	164	251	120	256	258	158.1	147	159	194
Th	41.3	56	55	38.7		52	54	41.7	137	64	51	43	49	56	35	69.5	39	44	43
U	7.3		11	6.1			13	4.9	46	13	14					14	67		14
La	103.5	181	101	112.7		106	249	137.7	66.9	388	106	205	116	152	203	78.2	133	137	134
Ce	208.6	348	209	172.7		209	393	290.5	261	340	260	368	229	308	409	166.5	263	296	268
Pr	24.04	42.5	22.9	29.53		25.1	56.8	32.47	15.7	76.4	22.2	49.3	27	36.7	54.1	19.59	30.7	34.1	34.3
Nd	90.3	137	69	110.7		81.5	188	118.8	42.4	224	64.7	159	85.6	116	173	71.8	101	108	118
Sm	17.5	29.8	14.5	19.6		16.5	44.6	21.2	8.2	43.5	13.2	36.1	18	25.1	40.8	15.9	20.3	23.9	25.3
Eu	2.04	3.86	1.85	2.81		2.36	4.11	2.53	0.85	5.44	1.69	4.14	2.53	2.9	5.68	0.79	2.72	2.78	3.74
Gd	19.59	32.5	15	16.56		17.8	52.8	18.64	6.7	47.6	14.4	40.6	18.9	28.5	45.7	16.64	21.7	25.7	28.6
Tb	4.14	5	2.49	3.17		2.83	9.49	3.61	1.17	7.81	2.55	6.54	3.12	4.74	7.59	3.6	3.52	4.28	4.69
Dy	24.93	27.4	14.9	17.35		16.6	55.8	19.8	6.78	44.1	15.6	38.3	18.1	29.1	43	20.37	20.3	25.1	27.5
Ho	5.71	5.59	3.03	3.5		3.51	10.8	3.88	1.39	9.16	3.3	7.73	3.86	6.55	8.73	4.64	4.28	5.17	5.76
Er	17.51	15.9	9.11	11.1		10.5	28.6	11.28	4.14	25.9	10.1	22.6	11.4	20.1	25.1	14.24	13	15.7	16.1
Tm	2.59	2.24	1.39	1.72		1.57	3.52	1.62	0.66	3.81	1.54	3.25	1.74	3.08	3.71	2.18	1.9	2.29	2.38
Yb	15.34	13.8	9.1	11.24		10	23.6	10.24	4.2	22.9	9.5	20.5	11	18.5	22.8	14.51	12.4	14.6	15.1
Lu	2.06	2.13	1.3	1.66		1.46	3.19	1.42	0.61	3.3	1.37	2.99	1.61	2.84	3.29	2.1	1.83	2.13	2.2
F	1090	2493	1431	2230	103	1416	2364		275	1257	3268	1266	1090	1484		710	1090	685	1394
W	1.1		12	1.2				1.2		14	15				16	1.8	19		10
Sn	16		6				13	10		6	122					17	6		
Mo	1.9			1.8				3.6								2.4			

Sample	sj16	1727	1715	1723	1731	1800a	1799	sj36a	sj18	sj07	1714	1859	sj06	sj09	1716	1823a	sj29	1809	sj1718
SiO_2	72.80	72.90	73.00	73.00	73.00	73.00	73.10	73.10	73.40	73.50	73.60	73.70	73.70	73.80	73.90	73.90	74.00	74.10	74.10
TiO_2	0.44	0.61	0.51	0.16	0.23	0.51	0.54	0.58	0.38	0.50	0.56	0.50	0.51	0.52	0.47	0.19	0.49	0.50	0.48
Al_2O_3	11.60	11.80	11.90	14.60	14.00	12.10	11.90	11.70	12.30	12.20	12.00	11.90	12.30	12.10	11.90	13.50	12.00	11.90	12.20

Fe$_2$O$_3$	1.77	2.59	2.14	1.00	0.62	1.83	2.36	2.66	1.77	2.21	1.51	1.39	2.65	1.02	1.65	0.89	0.54	1.81	1.41
FeO	2.57	2.55	2.54	0.79	2.34	2.63	2.35	2.84	1.94	1.86	3.21	2.47	1.77	2.91	2.50	1.78	4.12	2.58	3.08
MnO	0.04	0.06	0.07	0.01	0.03	0.02	0.06	0.05	0.03	0.02	0.08	0.03	0.02	0.03	0.05	0.02	0.07	0.06	0.06
MgO	0.40	0.53	0.52	0.28	0.24	0.80	0.52	0.49	0.43	0.76	0.51	0.87	0.75	2.15	0.42	0.30	0.46	0.49	0.45
CaO	1.20	1.78	1.46	0.59	1.33	0.56	1.24	1.09	1.18	0.93	1.40	0.67	1.19	1.12	1.17	0.79	1.50	1.23	1.48
Na$_2$O	2.80	2.50	3.00	3.60	3.20	6.10	2.30	2.30	3.00	3.60	2.70	2.70	3.80	3.20	2.80	3.10	2.80	2.40	2.70
K$_2$O	4.50	4.70	4.40	6.00	5.80	0.69	5.20	5.60	5.30	4.30	5.00	5.30	3.50	2.30	4.60	5.40	4.50	5.20	5.20
P$_2$O$_5$	0.08	0.12	0.11	0.09	0.04	0.10	0.11	0.12	0.07	0.11	0.11	0.11	0.12	0.07	0.10	0.07	0.10	0.12	0.09
LOI		0.10	0.24	0.23		0.17	0.06	0.40			0.26	0.12	0.09	0.71	0.11	0.29	0.17		1.34
Total	98.20	100.14	99.75	100.36	101.06	98.34	99.85	100.59	100.20	99.99	100.94	99.76	100.40	99.93	99.67	100.23	100.75	101.73	101.25
Cr																			
Ni																			
Co																			
V	13	21	27			20	21	18	10	15	20	12	11	18	12	10	22	16	12
Cu																			
Pb																			
Zn																			
Rb	218	169	223	343	357	20	216	268	252	217	141	238	127	229	219	351	201	203	206
Cs																			
Ba	1128	1304	1222	608	1065	353	1281	1430	846	953	1400	1485	1051	525	1007	546	1080	1214	1102
Sr				47	21		10				24		13	11		6			
Ga	21	20	15	23	21	23	22	17	20	20	17	20	20	17	18	21	22	19	16
Ta																			
Nb	68	114	66	25	40	75	75	68	54	79	57	65	68	69	60	42	77	67	56
Hf																			
Zr	555	693	596	176	320	612	560	607	400	683	636	661	628	759	600	191	614	580	505
Y	164	201	164	235	136	143	232	297	134	227	111	168	189	293	264	173	190	192	125
Th	60	32	56	73	50	55	53	35	58	53	31	45	44	81	37	69	60	36	53
U				30				12							10		16		
La	129	148	148	73.8	77.5	122	153	200	95	106	103	150	201	221	187	79.7	133	116	135
Ce	271	315	315	130	155	265	293	382	201	218	223	301	346	193	256	171	281	254	284
Pr	31.1	37.6	37.2	17	17	31.3	35.9	50.4	22.7	26.7	26.1	34.1	48	56.2	38.7	20.7	32.7	29.1	32.2
Nd	104	121	120	55.1	51.2	105	119	167	72.7	90.5	85.6	106	153	158	130	64.3	107	92.9	100
Sm	20.9	28	26.4	13.8	10.9	22.1	25.1	40.3	14.8	22.3	18.9	23.8	32.5	35.3	28.4	16.2	22.6	22.9	20.9
Eu	2.46	2.87	3.03	1.19	2.01	2.82	3.01	4.87	1.94	3.09	2.8	2.69	4.33	3.5	4.03	1	2.52	2.27	2.49
Gd	22.8	30	28.1	17.5	11.5	23.9	28.3	48.3	15.5	24.4	20.5	26	31.4	34.3	38.8	17.5	24.2	25.6	21.1
Tb	3.76	5.25	4.5	3.28	2	3.94	4.76	7.9	2.67	4.18	3.34	4.24	5.43	6.51	6.18	3.15	4.01	4.6	3.36
Dy	22.1	31.4	25.5	20.9	12.1	22.7	29	44	16.2	25.6	19.4	25.2	31.3	39.6	34.6	19.5	24.1	28.3	18.8
Ho	4.57	6.59	5.19	4.79	2.61	4.68	6.25	8.71	3.48	5.51	4.03	5.06	6.31	8.23	7.08	4.19	5.17	5.93	3.9
Er	13.3	19.3	14.5	14.6	8.05	13.6	19.1	23.4	10.5	16.9	11.9	14.5	18.6	24	18.6	12.7	15.4	17.3	10.9
Tm	1.95	2.89	2.09	2.22	1.26	2.08	2.94	3.26	1.59	2.55	1.69	2.19	2.51	3.57	2.49	1.91	2.37	2.46	1.57
Yb	12.2	17.5	13.6	14.4	8.6	13.1	19.1	19.8	10.4	16.6	11.4	13.5	16.8	23	14.9	12.9	15.6	14.5	9.9
Lu	1.72	2.4	1.96	2.16	1.21	1.86	2.94	2.72	1.59	2.45	1.63	2.01	2.38	3.26	2.06	1.92	2.34	2.01	1.45
F	480	638	1283	211	1600	410	1043	3206	1071	1278	1042	1523	1240	2799	725	439	1526	471	1202
W	27					12	25	11	10		22			15	16	10			12
Sn			11					18											
Mo																			

Sample	sj26b	sj19	1823bdup	sj08a	1470	sj17	1822	sj21	1456	sj13	sj03	1823b	20	1809djoc	1978joc	1445
SiO$_2$	74.10	74.20	74.70	74.90	75.00	75.20	75.30	75.40	75.60	75.60	75.70	75.80	75.90	76.34	76.80	77.10
TiO$_2$	0.53	0.34	0.29	0.49	0.14	0.47	0.11	0.35	0.30	0.45	0.11	0.29	0.21	0.18	0.15	0.19
Al$_2$O$_3$	12.00	12.00	12.20	11.70	13.60	12.10	13.50	12.50	11.20	11.70	13.50	12.20	11.70	11.67	12.38	12.20
Fe$_2$O$_3$	2.24	1.58	1.43	1.74	0.66	1.07	0.77	0.45	2.04	1.21	0.66	1.43	0.40	2.01	2.31	0.74
FeO	2.68	1.77	2.44	2.90	0.99	2.34	0.99	3.00	1.22	2.92	1.21	2.44	0.99	0.96	0.90	1.98
MnO	0.04	0.05	0.02	0.03	0.02	0.02	0.01	0.04	0.02	0.03	0.03	0.02	0.02	0.03	0.01	0.03
MgO	0.49	0.34	0.36	0.30	0.30	1.39	0.28	0.35	0.26	0.30	0.22	0.36	0.23	0.13	0.30	0.15
CaO	1.47	1.21	0.87	0.90	1.11	0.87	0.97	1.30	0.42	0.69	0.69	0.87	0.88	0.48	0.54	0.49

Table 2 (*continued*)

Sample	sj26b	sj19	1823bdup	sj08a	1470	sj17	1822	sj21	1456	sj13	sj03	1823b	20	1809djoc	1978joc	1445
Na_2O	2.80	2.90	3.10	2.50	3.00	4.70	3.70	3.10	2.60	2.30	3.50	3.10	2.80	2.29	6.59	2.80
K_2O	4.10	5.10	4.20	4.70	5.70	2.30	5.00	4.70	5.10	4.50	5.20	4.20	5.70	6.08	0.44	5.70
P_2O_5	0.11	0.06	0.06	0.08	0.04	0.11	0.04	0.06	0.02	0.07	0.04	0.06	0.01	0.05	0.17	
LOI	0.12	0.12	0.07		0.25	0.13	0.17	0.22	0.06	0.28	0.25	0.07	0.18	0.60	0.30	0.03
Total	100.68	99.67	99.74	100.24	100.81	100.70	100.84	101.47	98.84	100.05	101.11	100.84	99.02	100.82	100.89	101.41
Cr														*	*	
Ni														16.2	13.9	
Co														1.6	3.3	
V	23			18		11		15		11		16		7	5	
Cu														2.5	5.7	
Pb														14.2	6.3	
Zn														27	10	
Rb	236	163	259	143	252	86	272	191	193	171	487	250	205	193.5	23.5	385
Cs														0.3	0.3	
Ba	964	894	511	1035	390	590	384	658	766	1052	201	501	438	1017.7	270.4	323
Sr	11		13		24		47	29		38	7	19		77	32.4	
Ga	20	18	24	20	20	21	22	19	15	14	26	20	17	18.5	22.3	21
Ta	18					10								1.2	4.7	
Nb	71	58	49	36	12	71	16	55	42	50	49	40	76	21.1	45.8	101
Hf														5.7	5.4	
Zr	631	466	481	701	113	673	130	390	466	394	96	444	419	167.3	138.6	331
Y	198	187	154	52	118	146	101	133	86	89	151	141	189	93.1	51.9	160
Th	55	45	85	34	54	49	58	73	117	5	36	77	95	27.4	17.9	118
U									15	10	14	11	10	5.4	19.5	19
La	172	144		67.4	62.7	120	57.8	144	75.5	84.1	42	106	154	100	25.9	91.3
Ce	374	219		167	132	255	121	292	164	249	83.6	234	309	189.4	54.2	174
Pr	45	30.2		16.1	16.3	30	14.8	31.4	20	23.6	10.9	28.1	36.2	22.19	6.27	21.2
Nd	143	94.3		49.9	50.2	96.1	44.7	92.5	58.2	76.6	33.1	86.7	113	78.1	23.3	65.1
Sm	30.7	20.2		9.6	13	22	11.3	18.1	11.3	18	8.9	20.2	22.9	14.7	5.3	14.9
Eu	3.91	2.25		1.4	1.08	2.96	0.71	1.69	1.04	2.11	0.4	1.17	0.84	1.8	0.84	1.24
Gd	31.2	21.6		9.64	12.5	23.3	10.8	18.5	9.37	18.6	8.61	19.2	24.6	13.72	5.93	15.8
Tb	4.99	4		1.53	2.45	3.78	1.98	3.06	1.79	3.13	1.8	3.52	4.11	2.83	1.29	2.9
Dy	28.5	24.6		7.94	15.6	21.9	11.6	18.3	11	18.9	11.4	21	23.6	15.51	7.94	17.7
Ho	5.84	5.4		1.58	3.44	4.56	2.39	3.81	2.29	3.87	2.33	4.34	5.03	3.08	1.63	3.85
Er	17.2	15.7		4.24	10.8	13.3	7.09	11.6	6.85	11.4	7.35	12.7	15.1	8.96	5.4	11.7
Tm	2.42	2.18		0.58	1.5	2	0.99	1.71	1.02	1.73	1.06	1.77	2.4	1.22	0.83	1.86
Yb	15.4	14.9		3.5	10.4	12.8	7.1	11.2	7.4	11.4	8	12.7	15.4	6.82	5.44	11.7
Lu	2.22	2.07		0.51	1.49	1.86	0.96	1.67	1.04	1.63	1.21	1.8	2.24	0.95	0.84	1.71
F	1923	479	447	344	156	2158	286	602	289	248	466	475	2487	120	580	686
W	12					13		17	14					1.4	1.6	
Sn				5									14	4	5	
Mo														1.8	2.9	

ar o que significa; células em branco: colocar o que significa.
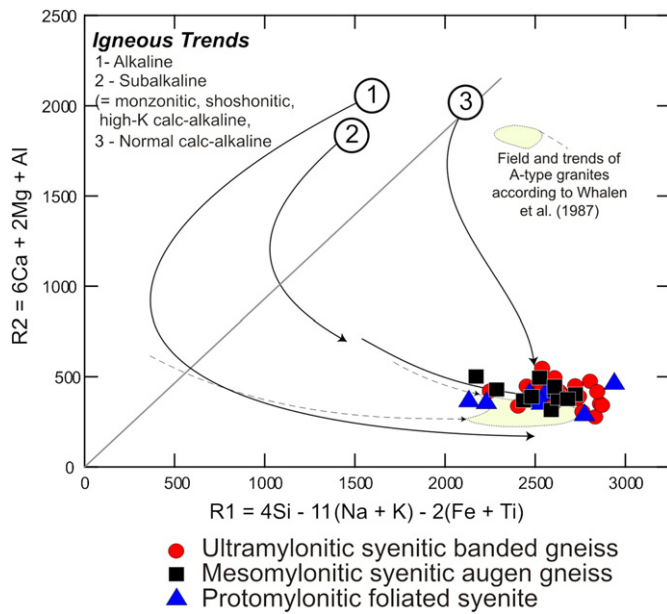
Fig. 5. R1–R2 diagram, modified from De La Roche et al. (1980), showing normal calc-alkaline, subalkaline and alkaline trends and the locations of the A-type granitoid samples, according to Whalen et al. (1987). The samples are distributed in the more differentiated part of the subalkaline trend, partly overlapping the A-type granitoids field.

which distinguishes A1-type granitoids, produced by fractional crystallization of mantle material, from A2-type granitoids with strong crustal contamination. The Caraguataí orthogneisses plot in the A2 granitoids field, considered by many authors as emplacing in late, post-collisional settings (Best, 2003).
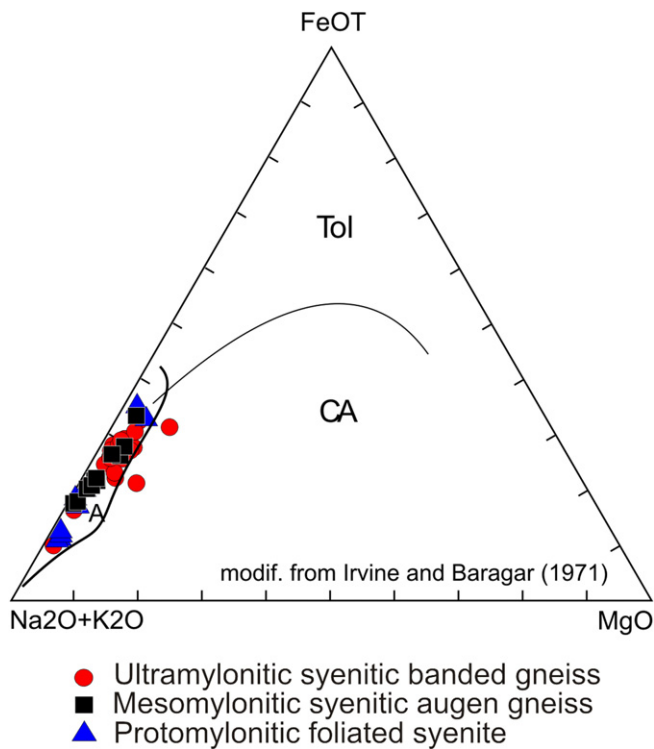
Fig. 6. AFM diagram of Irvine and Baragar (1971) with the A-type granitoids field of Whalen et al. (1987). Almost all samples are positioned within the A-type granitoids field.
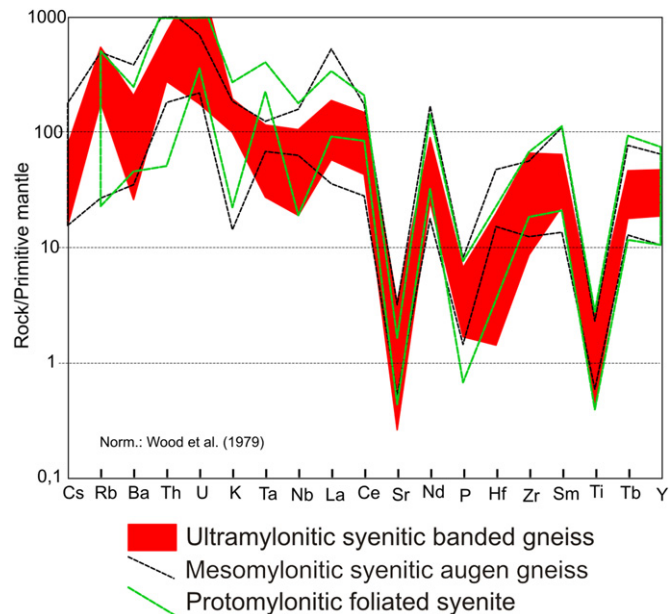
Fig. 7. Spiderdiagrams normalized to primordial mantle values (Wood et al., 1979) with compositional envelopes of the three lithofacies sampled.

In summary, the Caraguataí suite is composed of instead of by orthogneisses whose protoliths where metaluminous to per-aluminous, Fe-rich, integrating an A2-type magmatism, characterized as alkaline by means of mineral composition and trace element contents. They resulted from partial melting of an igneous continental crust in a high geothermal grade and low pressure setting (less than 15 km deep) where plagioclase was a stable phase. Such scenario is compatible with non-compressional settings, in the presence of intense mafic magmatism.

3.2. U–Pb and Sm–Nd geochronology

U–Pb on zircon analyses were performed by in situ LA-ICPMS measurements and Sm–Nd model ages (T_{DM}) were calculated from TIMS analyses. The locations of the samples used are plotted
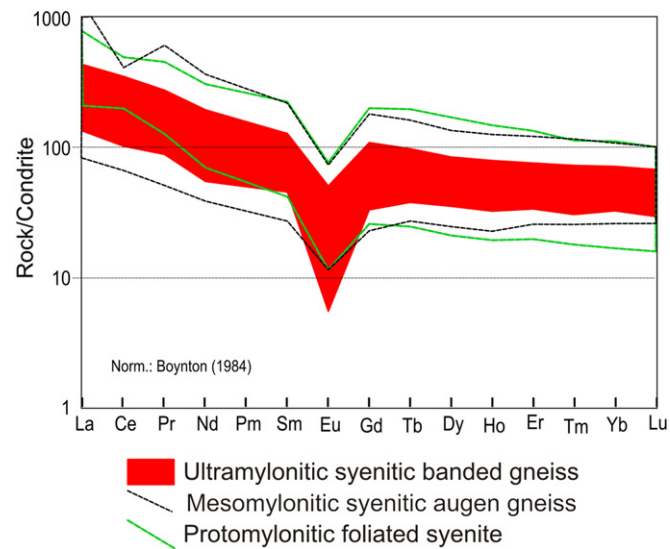
Fig. 8. REE patterns with compositional envelopes of the three rock types sampled.

Fig. 9. Pearce's (1996) discrimination diagram for tectonic environments.

Fig. 10. Eby's (1992) diagram. A1: field for a purely mantle magmatic origin and A2: field for a magmatic or crustal origin with products resulting from mantle−crust interaction. Samples from Suite Caraguataí fall in the A2 field.
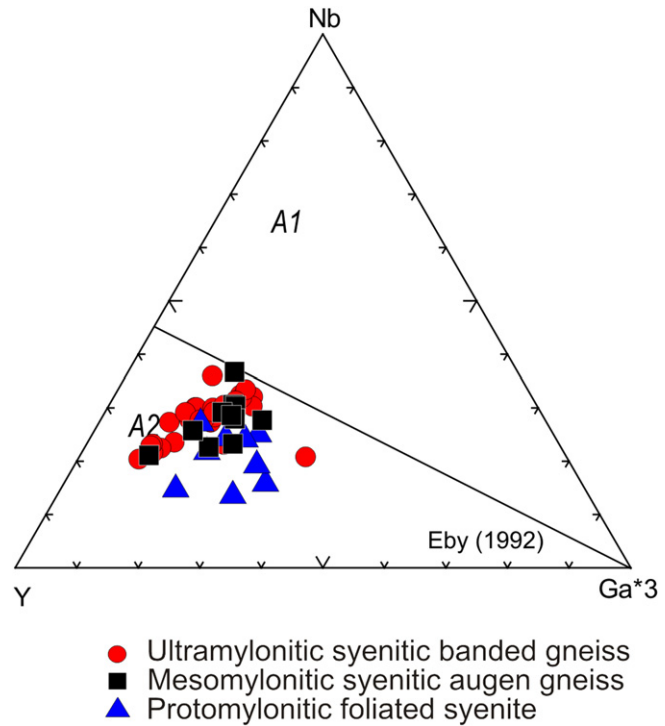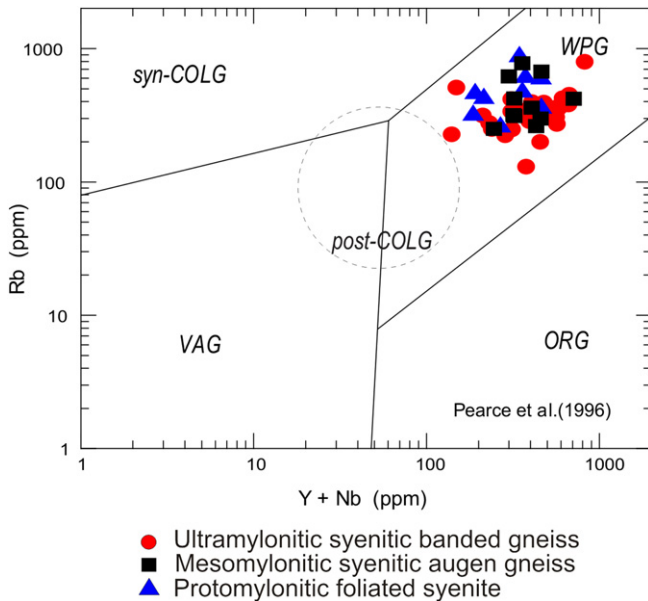
in Fig. 3 and the data obtained are listed in Tables 3 and 4. Crushing and mineral separation were performed in Sample Preparation Laboratory of the OuroPreto Federal University. Isotope analyses were performed in the Laboratory of Geochronology of the University of Brasilia according to the methodology described in Gioia and Pimentel (2000) and Buhn et al. (2009). The errors were calculated with the Isoplot 3 program of Ludwig (2003) and quoted at the 2 sigma level.

3.2.1. U−Pb geochronology

Five rock samples from the Caraguataí Suite showing distinct degrees of deformation were chosen and dated using the in situ LA-ICPMS method. The results are listed in Table 3.

Sample SCP 1470 is an undeformed syenite. Zircon grains are euhedral, brown, often metamictic and of the S25-J5 alkaline types of Pupin (1980) (Fig. 11). Only 5 analyses provided usable results and define an intercept at 2678 ± 23 Ma ($\pm 2\sigma$, MSWD = 4.4) and a weighted average of ^{207}Pb/^{206}Pb ages of 2680 ± 24 Ma. The ages calculated are similar to those obtained for sample SCP 2035 (see below) with a higher error, related to a scattering of the data in the concordia diagram.

Sample SCP 2035 is a foliated syenite. Zircon crystals are euhedral, clearly magmatic and with a fine concentric zoning. They are of the S25-J5 types of Pupin (1980) and typical of high temperature alkaline magmas (Fig. 12). Out of twenty analyses performed (Table 3), two grains exhibit discordant U/Pb ratios (9 and 20) and two other (13 and 14) yielded ^{207}Pb/^{206}Pb ages significantly younger than the rest of the data. Using the whole data set, the 20 analyses define an intercept age of 2694 ± 15 Ma ($\pm 2\sigma$, MSWD = 2.4) and a weighted average ^{207}Pb/^{206}Pb age of 2701 ± 11 Ma. Using the 16 best analyses, we obtained an intercept age of 2700 ± 7 Ma (MSWD = 1.2) and a mean ^{207}Pb/^{206}Pb age of 2703 ± 11 Ma (MSWD = 2.1). The age of ca. 2.70 Ga is interpreted as that of the syenitic magmas.

Sample SCP 1446 is a mesomylonitic syenitic augen gneiss. Zircon crystals are pink, euhedral and very finely zoned; instead of, they are often of the J5 type, also typical of alkaline magmas (Fig. 13). A set of 19 data (out of twenty) allows to define an intercept at 2711 ± 26 Ma (MSWD = 0.09) with a weighted

average of ^{207}Pb/^{206}Pb ages of 2711 ± 31 Ma (MSWD = 0.04). The low MSWD value is related to the high individual analytical errors on the U/Pb ratios (see Table 3). Grain Z19 is older with a ^{207}Pb/^{206}Pb discordant age at ca. 2.96 Ga. It is a skeletal grain and even if it contains more common lead, it is probably inherited.

Sample SCP 1809 is also an ultramylonitic syenitic banded gneiss. Zircon grains are euhedral and of the S25-J5 types of Pupin (1980) (Fig. 14). Results are more complex than the previous ones, with three sets of ages. One analysis (Z22, Table 3), with a ^{207}Pb/^{206}Pb age ca. 2.03 Ga, is not reported in Fig. 14 because it falls totally out of the main set, even if the zircon is a typical alkaline grain. This grain could have been reset during the emplacement of the surrounding Paleoproterozoic Jussiape granite. A second set of three results is sub-concordant (Z1-21 and 24) and have ^{207}Pb/^{206}Pb ages of ca. 2.64 Ga, which is significantly younger than the main set of ca. 2.7 Ga. These grains are also typical of alkaline magmas. They could be the witness of a metamorphic event but the age is probably not significant and might correspond to a restricted Pb loss from the magmatic set. The last and main set of 21 data is in part concordant and in part discordant. The 21 analyses define an intercept age of 2691 ± 14 Ma (MSWD = 4.2). The 11 concordant points define a mean ^{207}Pb/^{206}Pb age of 2697 ± 13 Ma (MSWD = 3.9) which is probably the most reliable for this sample. The high MSWD indicates some disturbance of the U−Pb system, even if it is restricted.

Sample SCP 2017 is a mesomylonitic syenitic augen gneiss. Zircon grains are beautifully prismatic and euhedral with fine concentric zoning and typical of alkaline magmas (Pupin, 1980) (Fig. 15). A set of 17 analyses out of 20 defines an intercept at 2706 ± 24 Ma (MSWD = 0.06) and a mean ^{207}Pb/^{206}Pb age of 2706 ± 34 Ma (MSWD = 0.03).

The Caraguataí syenitic suite constitutes a single unit in the field and from instead of on a geochemical point of view. This is in

Table 3
Summary of LA-ICPMS U–Pb zircon results. Uncertainties are given at the 1σ level. (−) Parameter not analyzed.

	Th/U	Isotopic ratios							Rho	Ages in Ma						Conc
		$^{206}Pb/^{204}Pb$	$^{207}Pb/^{206}Pb$	±1σ (%)	$^{207}Pb/^{235}U$	±1σ (%)	$^{206}Pb/^{238}U$	±1σ (%)		$^{207}Pb/^{235}U$	±1σ (%)	$^{206}Pb/^{238}U$	±1σ (%)	$^{207}Pb/^{206}Pb$	±1σ (%)	(%)
Sample SCP 1470																
Z1	–	–	0.1811	0.7	12.817	1.2	0.5132	1.1	0.92	2666	12	2670	23	2663	27	100
Z2	–	–	0.1831	0.9	13.428	1.2	0.5318	1.1	0.90	2710	13	2749	24	2681	29	98
Z6	–	–	0.1852	0.7	13.039	1.0	0.5106	0.9	0.89	2682	11	2659	19	2700	24	102
Z7	–	–	0.1822	1.5	12.080	1.7	0.4807	1.5	0.89	2611	20	2530	32	2673	44	106
Z8	–	–	0.1820	0.8	13.404	1.0	0.5341	0.9	0.90	2709	11	2759	21	2671	25	97
Sample SCP 2035																
Z1	0.28	6635	0.1893	1.0	11.576	1.6	0.4436	1.2	0.72	2571	15	2367	25	2736	17	86
Z2	0.42	54,050	0.1859	0.9	13.033	1.4	0.5084	1.0	0.68	2682	13	2650	22	2706	15	98
Z3	0.22	7681	0.1835	1.1	13.129	3.0	0.5189	2.8	0.94	2689	28	2695	61	2685	17	100
Z4	0.30	8951	0.1869	1.1	11.744	3.9	0.4556	3.8	0.93	2584	37	2420	77	2715	18	89
Z5	0.28	20,521	0.1828	0.9	12.651	1.9	0.5018	1.7	0.88	2654	18	2622	36	2679	15	98
Z6	0.26	59,061	0.1863	0.8	14.261	4.0	0.5553	3.9	0.98	2767	38	2847	89	2709	14	105
Z7	0.38	54,323	0.1849	0.8	13.859	1.8	0.5435	1.6	0.90	2740	17	2798	37	2698	13	104
Z8	0.24	16,558	0.1837	1.2	13.201	3.4	0.5213	3.2	0.88	2694	32	2705	71	2686	20	101
Z9	0.26	18,358	0.1881	1.1	9.289	2.4	0.3582	2.1	0.90	2367	22	1974	37	2725	17	72
Z10	0.30	146,291	0.1834	1.0	13.469	1.4	0.5326	1.0	0.68	2713	13	2752	22	2684	16	103
Z11	0.37	68,737	0.1807	1.0	13.304	1.5	0.5341	1.2	0.73	2701	15	2759	26	2659	17	104
Z13	0.29	37,060	0.1778	1.4	11.754	1.7	0.4794	1.1	0.59	2585	16	2525	23	2633	23	96
Z14	0.29	45,070	0.1799	1.2	11.919	1.6	0.4807	1.1	0.65	2598	15	2530	22	2652	19	95
Z17	0.30	87,028	0.1876	0.9	13.331	1.2	0.5153	0.8	0.57	2703	11	2679	18	2722	14	98
Z18	0.37	117,633	0.1873	0.8	13.730	1.4	0.5318	1.1	0.82	2731	13	2749	25	2718	13	101
Z19	0.09	63,375	0.1896	0.8	11.809	1.5	0.4517	1.3	0.86	2589	14	2403	26	2739	12	88
Z20	0.11	68,313	0.1762	3.1	9.364	5.2	0.3854	4.2	0.79	2374	48	2101	76	2618	52	80
Z22	0.18	53,388	0.1855	0.8	13.183	1.3	0.5154	1.0	0.73	2693	12	2680	22	2703	14	99
Z23	0.22	252,558	0.1840	0.7	13.798	1.2	0.5438	0.9	0.77	2736	11	2800	21	2689	12	104
Z24	0.28	29,896	0.1837	0.9	13.860	2.2	0.5471	2.0	0.82	2740	21	2813	46	2687	15	105
Sample SCP 1446																
Z1	0.43	24,536	0.1888	4.8	11.816	6.8	0.454	4.7	0.90	2590	63	2413	96	2732	79	88
Z2	0.27	5897	0.1900	5.6	13.234	7.9	0.505	5.5	0.91	2697	74	2636	120	2742	92	96
Z3	0.31	20,285	0.1835	3.7	12.711	5.2	0.502	3.6	0.86	2658	49	2624	77	2685	61	98
Z4	0.36	21,376	0.1881	5.2	13.099	7.3	0.505	5.1	0.92	2687	69	2635	111	2726	86	97
Z5	0.39	17,207	0.1874	4.1	12.852	5.7	0.497	3.9	0.85	2669	53	2602	84	2720	67	96
Z6	0.33	10,449	0.1868	4.4	12.757	6.2	0.495	4.4	0.88	2662	59	2593	93	2714	73	96
Z7	0.34	26,687	0.1873	3.7	12.982	5.1	0.503	3.6	0.86	2678	48	2625	77	2719	61	97
Z8	0.27	22,585	0.1869	4.8	12.984	6.8	0.504	4.8	0.91	2678	64	2631	103	2715	80	97
Z9	0.57	31,521	0.1866	4.1	10.167	5.8	0.395	4.0	0.88	2450	53	2147	74	2712	68	79
Z10	0.36	35,262	0.1873	3.9	12.909	5.4	0.500	3.8	0.87	2673	51	2613	81	2718	64	96
Z11	0.28	72,671	0.1855	3.7	10.503	5.2	0.411	3.6	0.86	2480	48	2217	68	2703	62	82
Z12	0.33	31,791	0.1842	4.0	13.267	5.5	0.522	3.8	0.85	2699	52	2710	83	2691	65	101
Z13	0.36	26,311	0.1876	3.8	13.576	5.2	0.525	3.6	0.86	2721	50	2720	80	2721	62	100
Z14	0.37	25,840	0.1865	3.9	13.890	5.4	0.540	3.8	0.88	2742	51	2784	86	2712	64	103
Z15	0.41	26,298	0.1871	5.2	12.947	7.3	0.502	5.1	0.93	2676	69	2621	110	2717	85	96
Z16	0.20	42,699	0.1853	4.3	13.323	6.0	0.522	4.2	0.87	2703	56	2706	92	2701	71	100
Z17	0.12	46,094	0.1876	3.8	14.202	5.3	0.549	3.7	0.87	2763	51	2821	85	2721	63	104
Z18	0.31	33,919	0.1842	4.0	13.161	5.5	0.518	3.8	0.87	2691	52	2692	84	2691	65	100
Z19	0.24	1780	0.2174	7.1	16.262	10.0	0.543	7.1	0.89	2892	96	2795	160	2961	115	94
Z20	0.31	52,763	0.1861	4.0	13.529	5.4	0.527	3.7	0.83	2717	51	2730	81	2708	66	101
Sample SCP 1809																
Z1	0.15	82,993	0.1803	0.51	12.227	1.09	0.4919	0.96	0.75	2622	10	2579	20	2656	8	97
Z2	0.29	97,041	0.1838	0.51	13.398	1.20	0.5287	1.08	0.79	2708	11	2736	24	2687	8	102
Z3	0.21	561	0.1843	1.37	11.313	1.78	0.4453	1.13	0.65	2549	16	2374	22	2692	22	88
Z4	0.24	86,983	0.1848	0.56	13.355	1.34	0.5241	1.22	0.75	2705	13	2717	27	2696	9	101
Z5	0.16	–	0.1893	0.66	10.281	2.12	0.3939	2.02	0.86	2460	19	2141	37	2736	11	78
Z6	0.33	40,656	0.1880	0.69	13.259	1.60	0.5116	1.44	0.81	2698	15	2663	31	2725	11	98
Z7	0.22	58,544	0.1851	0.53	12.885	1.29	0.5048	1.18	0.80	2671	12	2634	26	2699	9	98
Z8	0.23	–	0.1870	0.63	13.145	1.13	0.5099	0.94	0.73	2690	11	2656	20	2716	10	98
Z9	0.19	94,269	0.1868	0.59	13.598	0.99	0.5278	0.79	0.70	2722	9	2732	18	2715	10	101
Z10	0.17	15,377	0.1824	1.49	11.527	2.14	0.4584	1.53	0.69	2567	20	2432	31	2675	25	91
z11	0.18	450	0.1919	0.87	14.749	1.77	0.5576	1.54	0.75	2799	17	2857	35	2758	14	104
Z12	0.25	112,577	0.1864	0.58	13.316	1.79	0.5180	1.69	0.84	2702	17	2691	37	2711	9	99
z13	0.20	2,615,498	0.1859	0.58	12.006	1.30	0.4685	1.16	0.76	2605	12	2477	24	2706	10	92
Z14	0.04	46,394	0.1783	0.55	13.583	1.66	0.5523	1.57	0.83	2721	16	2835	36	2638	9	107
z15	0.19	62,872	0.1832	0.73	13.111	2.41	0.5190	2.30	0.81	2688	23	2695	50	2682	12	100
Z16	0.19	59,697	0.1818	0.65	12.961	1.80	0.5170	1.68	0.82	2677	17	2686	37	2670	11	101
z17	0.17	80,972	0.1806	0.61	13.013	1.66	0.5226	1.54	0.81	2681	16	2710	34	2659	10	102
Z18	0.20	2,537,241	0.1861	0.66	14.054	1.59	0.5477	1.45	0.79	2753	15	2816	33	2708	11	104
Z19	0.20	58,176	0.1851	0.82	14.540	1.85	0.5697	1.66	0.77	2786	17	2907	39	2699	14	108
z20	0.21	107,875	0.1867	0.67	14.367	1.43	0.5582	1.27	0.74	2774	14	2859	29	2713	11	105

Table 3 (*continued*)

	Th/U	Isotopic ratios							Rho	Ages in Ma						Conc (%)
		$^{206}Pb/^{204}Pb$	$^{207}Pb/^{206}Pb$	$\pm1\sigma$ (%)	$^{207}Pb/^{235}U$	$\pm1\sigma$ (%)	$^{206}Pb/^{238}U$	$\pm1\sigma$ (%)		$^{207}Pb/^{235}U$	$\pm1\sigma$ (%)	$^{206}Pb/^{238}U$	$\pm1\sigma$ (%)	$^{207}Pb/^{206}Pb$	$\pm1\sigma$ (%)	
Z21	0.19	34,183	0.1785	0.63	12.338	1.25	0.5014	1.08	0.72	2630	12	2620	23	2639	10	99
z22	0.03	103,756	0.1248	0.90	6.739	1.63	0.3917	1.36	0.73	2078	14	2131	25	2026	16	105
Z23	0.22	114,779	0.1853	0.55	13.340	1.33	0.5223	1.21	0.77	2704	12	2709	27	2700	9	100
z24	0.19	93,607	0.1786	0.59	12.392	1.31	0.5033	1.17	0.76	2635	12	2628	25	2640	10	100
Z25	0.03	83,627	0.1813	0.53	15.783	1.58	0.6313	1.49	0.83	2864	15	3155	37	2665	9	118
Sample SCP 2017																
Z1	0.45	145,598	0.1856	4.4	12.235	6.4	0.4780	4.6	0.93	2623	60	2519	97	2704	72	93
Z2	0.40	86,117	0.1868	3.6	14.332	5.2	0.5564	3.8	0.90	2772	50	2852	88	2714	59	105
Z3	0.46	66,860	0.1872	4.2	12.402	6.0	0.4804	4.3	0.91	2635	56	2529	89	2718	69	93
Z4	0.31	177,785	0.1867	4.2	13.825	6.0	0.5370	4.2	0.89	2738	57	2771	96	2713	70	102
Z5	0.28	19,765	0.1852	5.2	12.595	7.3	0.4931	5.1	0.91	2650	69	2584	110	2700	85	96
Z6	0.16	9986	0.1859	4.8	12.691	6.8	0.4951	4.8	0.90	2657	64	2593	102	2706	79	96
Z7	0.26	13,652	0.1852	4.9	12.876	6.9	0.5041	4.9	0.91	2671	65	2631	106	2700	81	97
Z8	0.55	616	0.1939	5.3	11.245	7.4	0.4206	5.2	0.92	2544	69	2263	100	2775	86	82
Z9	0.33	291,919	0.1858	3.8	13.298	5.3	0.5192	3.7	0.88	2701	50	2696	82	2705	63	100
Z10	0.28	31,711	0.1886	3.8	13.197	5.4	0.5076	3.8	0.88	2694	51	2646	82	2730	63	97
Z11	0.40	42,914	0.1875	4.7	13.812	6.6	0.5344	4.7	0.92	2737	63	2760	105	2720	77	101
Z12	0.23	6563	0.1849	5.6	13.276	8.0	0.5209	5.6	0.92	2699	75	2703	125	2697	93	100
Z13	0.12	22,912	0.1710	4.0	10.820	5.6	0.4588	4.0	0.88	2508	52	2434	80	2568	66	95
Z14	0.27	12,955	0.1857	4.5	13.382	6.3	0.5226	4.4	0.91	2707	60	2710	98	2704	74	100
Z15	0.29	19,111	0.1832	4.9	12.606	6.9	0.4990	4.9	0.92	2651	65	2610	104	2682	81	97
Z16	0.33	61,505	0.1853	3.8	13.178	5.2	0.5158	3.6	0.86	2692	49	2681	79	2701	62	99
Z19	0.28	27,439	0.1839	4.1	12.551	5.7	0.4950	4.0	0.89	2647	54	2592	85	2688	68	96
Z18	0.23	53,982	0.1853	4.3	13.721	6.0	0.5371	4.2	0.90	2731	57	2771	95	2701	71	103
Z19	0.42	54,641	0.1856	4.9	13.726	6.9	0.5364	4.8	0.93	2731	65	2768	109	2704	81	102
Z20	0.15	25,975	0.1510	3.6	8.688	4.9	0.4172	3.4	0.85	2306	45	2248	65	2358	61	95

agreement with the ca. 2.7 ages obtained for the five samples ca. 2.7 Ga which are similar, taking into account the errors. We calculated an average for the 62 concordant analyses obtained from the five samples. A mean $^{207}Pb/^{206}Pb$ age of 2696 ± 5 Ma ($\pm2\sigma$, MSWD = 0.98) is obtained; instead of, it is interpreted as that of zircon growth in the syenitic magmas (Fig. 16). This age is also similar to the SHRIMP zircon age obtained for the alkaline Eixo gneisses, further south, at 2693 ± 5 Ma (Santos-Pinto et al., submitted for publication); they both indicate the occurrence of a major magmatic event ca. 2.7 Ga (see Discussion). The new geochronologic data do not help constrain an age for the metamorphism. New dating involving other mineral phases will be carried out in order to obtain the age of the metamorphic event that affected the Caraguataí Suite.

3.2.2. Sm–Nd results

Table 4 presents the results obtained for the five samples used for the U–Pb zircon dating. The Sm–Nd T_{DM} model ages were calculated using De Paolo's linear model (DePaolo, 1988), with an epsilon zero (DM0) value today of +8 and of +10, with a $^{147}Sm/^{144}Nd$ ratio of 0.2137 for the DM. Model ages range between 3.2 and 3.6 Ga with a DM0 of +8 and between 3.30 and 3.90 with a DM0 of +10. The εNd values at 2.7 Ga are negative and range between −4 and −6, suggesting crustal reworking processes. We reported in Fig. 17, in a Nd vs. time isotopic evolution diagram, the

isotopic growth lines for the five samples that plot in the evolution field defined for gneisses of the Gavião Block by Santos-Pinto et al. (submitted for publication).

4. Discussion

Data obtained during this work indicate that the Caraguataí pluton is a syenitic suite emplaced at ca. 2.7 Ga. No irrespective of the degree of deformation, from the undeformed facies to the ultramylonites zircon grains provide the same age with an average of 2696 ± 5 Ma for the 62 concordant analyses obtained from the five samples. This age is retained for this magmatic event. The strong shearing under amphibolite facies conditions observed in the various rock types did not significantly affect the U–Pb system of zircon and consequently we were not able to constrain the age of this shearing.

T_{DM} Nd model ages of the Caraguataí suite are in the range of those obtained for the surrounding Paleoarchean gneissic basement in the Umburanas-Brumado-Aracatu region (Santos-Pinto, 1996; Santos-Pinto et al., 1998, submitted for publication). Enriched mantle sources may have contributed to the genesis of these alkaline magmas and explain the negative epsilon(t) values (−4 to −6) observed, but these values seem to be too negative for the Archean where a depleted mantle model is often well constrained. Furthermore, taking into account that the

Table 4
Sm–Nd results for whole rocks of the Caraguataí suite. Coordinates from the geographic system WGS-84.

Sample	Coordinates	Modal composition	Tectonofácies	Sm (ppm)	Nd (ppm)	$^{147}Sm/^{144}Nd$	$^{143}Nd/^{144}Nd$ (2σ)	εNd$_{(t)}$	T_{DM} (Ga)
Caraguataí Suíte									
SCP 1446	24L/216831/8496234	Quartz syenite	Ultramilonitic	13.5	73.1	0.1121	0.510931 (15)	−4.0	3.22
SCP 2017	24L/210176/8520178	Quartz syenite	Augen mesomilonitic	16.6	94.7	0.1063	0.510776 (13)	−5.1	3.26
SCP 2035	24L/211687/8523483	Quartz syenite	Protomilonitic	16.6	77.5	0.1293	0.511149 (09)	−5.9	3.50
SCP 1470	24L/221668/ 8509740	Syenite	Isotropic	12.7	58.7	0.1311	0.511247 (18)	−4.73	3.39
SCP 1809	24L/217717/8509088	Quartz syenite	Ultramilonitic	14.7	56.1	0.1584	0.511718 (12)	−4.8	3.81
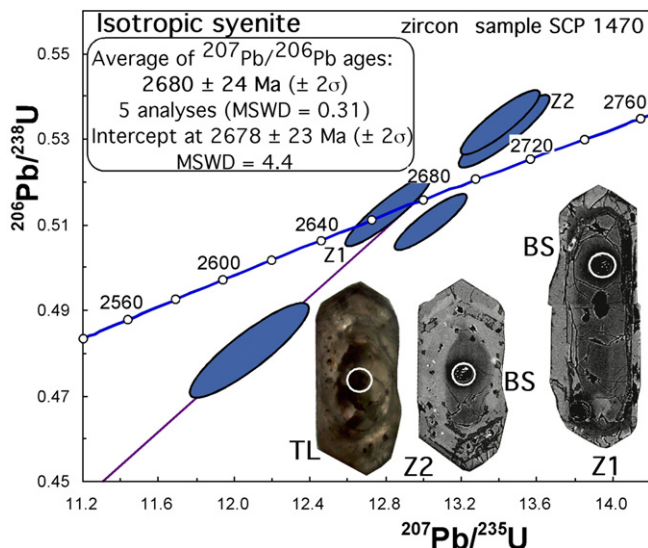
Fig. 11. Zircon U−Pb concordia plot for the isotropic syenite SCP 1470. TL = transmitted light and BS = backscattered images. White circles correspond to the laser spot (size ca. 20 μm). Ellipses are reported at 1σ.


Fig. 13. Zircon U−Pb concordia plot for the syenitic banded gneiss SCP 1446 (see images in Fig. 11). Ellipses are reported at 1σ.

magmatism is of the A2 type and the occurrence of some inherited zircon grains, the results seem to be better explained by the involvement of a Paleoarchean input which could be that recognized in the neighboring southern Aracatu region (Fig. 2) (Santos-Pinto et al., 1998, submitted for publication). Paleoarchean sources (>3.0 Ga) have also been found in other parts of the São Francisco Craton, as reported by Teixeira et al. (1996, 1998), Oliveira et al. (2000, 2002), Noce et al. (2007), for example. Such a Neoarchean magmatism is also known in the Aracatu region with the Serra do Eixo alkaline augen gneiss exhibiting a similar SHRIMP zircon age of 2693 ± 5 Ma and which is also derived from crustal melting of the surrounding Paleoarchean gray gneisses (Santos-Pinto et al., submitted for publication). Southwest of Brumado, the Guajeru alkaline granite provides a zircon age of ca. 2.66 Ga (Lopes, 2002, Table 1). In the Contendas Mirante region, the Pé de Serra alkaline to peralkaline gneiss corresponds

to a large deformed granitic to syenitic pluton. An aegirine-bearing syenite has a SHRIMP zircon age of 2652 ± 11 Ma (Marinho et al., 2008). Regionally, some older Archean gneisses, with zircon ages above 3.0 Ga (Santos-Pinto et al., 1998, submitted for publication), exhibit Rb−Sr ages of ca. 2.7 Ga (Table 1 and references within) which would also suggest the occurrence of a Neoarchean thermal event over 50 Ma between 2.70 and 2.65 Ga in this region.

In summary, the isotopic data obtained in this work and in the previous ones suggest a significant crustal recycling process has occurred at ca. 2.7 Ga in the southern part of the Gavião Block. It is evidenced by a significant subalkaline to alkaline magmatism which seems sporadically present within the Paleoarchean gneisses and were probably developed in an intraplate setting related to mantle upwelling, for example.
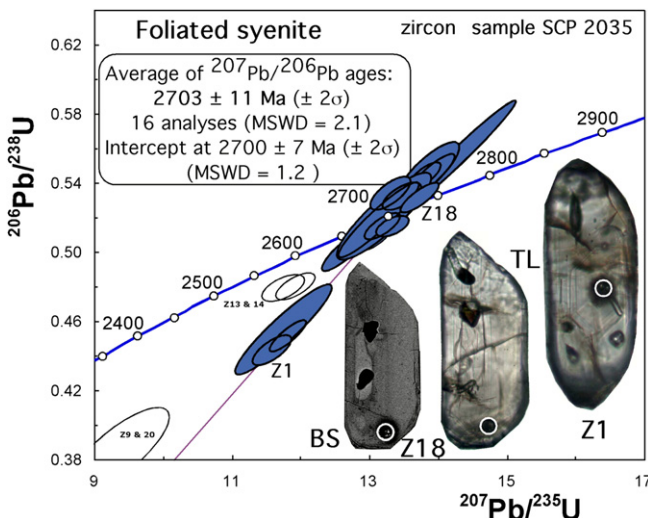
Fig. 12. Zircon U−Pb concordia plot for the foliated syenite SCP 2035 (see images − in Fig. 11). Ellipses are reported at 1σ.
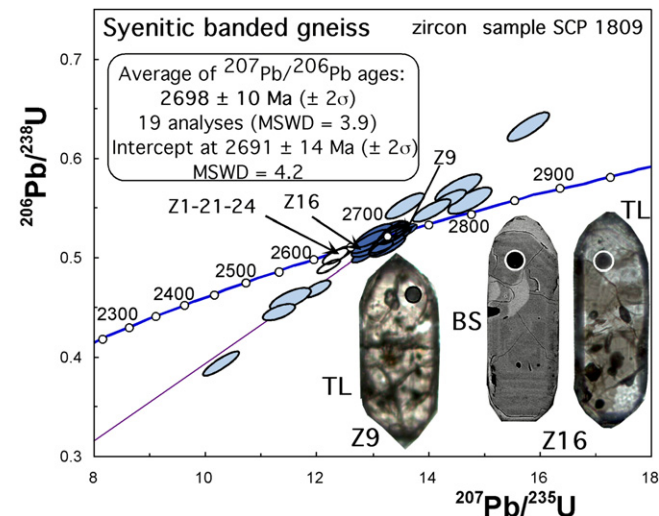
Fig. 14. Zircon U−Pb concordia plot for the syenitic banded gneiss SCP 1809 (see images in Fig. 11). Ellipses are reported at 1σ.
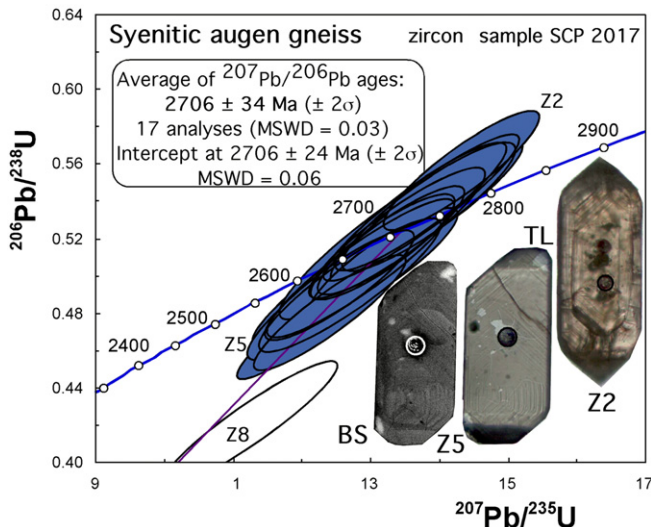
Fig. 15. Zircon U–Pb concordia plot for the syenitic augen gneiss SCP 2017 (see images in Fig. 11). Ellipses are reported at 1σ.
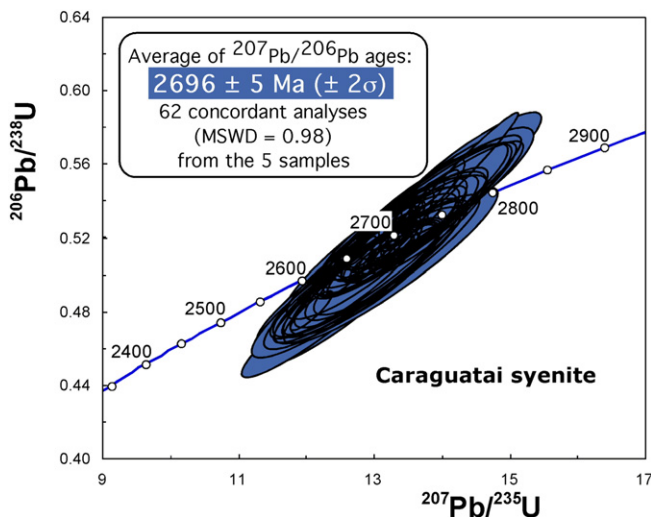
Fig. 16. Zircon U–Pb concordia plot for the 62 concordant analyses from the five samples of the Caraguataí syenitic suite. Ellipses are reported at 1σ.
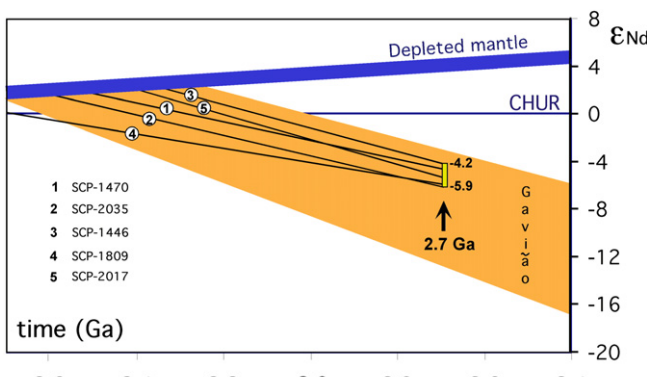

Fig. 17. Nd vs. time diagram for the five samples of the Caraguataí syenitic suite. Field for the Mesoarchean gneisses of the Gavião Block, after Santos-Pinto et al. (submitted for publication), is reported.

5. Conclusions

The Caraguataí intrusive suite comprises alkali-feldspar granites, syenites and quartz syenites. They are leuco- to mesocratic, pale gray and underwent several stages of deformation in shear zones to form protomylonites, augen-mesomylonites and ultra-mylonites. Chemical analyses suggest that the protoliths of these rocks are highly differentiated, potassic, metaluminous to per-aluminous, subalkaline to alkaline of the A2 type. U–Pb zircon ages defined for the five samples have similar ages of ca. 2.7 Ga which were not significantly disturbed by shearing processes. Sixty two concordant analyses from the five samples provide a mean $^{207}Pb/^{206}Pb$ age of 2696 ± 5 Ma, which is interpreted as that of the alkaline magmatism. These alkaline plutons were probably emplaced in an intraplate setting. The Nd Paleoarchean T_{DM} model ages (3.22–3.5 Ga) with the negative $\varepsilon_{Nd}(t)$ values (−4 and −6) indicate crustal reworking process of a Paleoarchean crust similar to that recognized in the southern Gavião block. Dating carried out up to now has not helped to constrain an age for the meta-morphism that affected the Caraguataí Suite. The isotopic data obtained in this work together with published data for the southern sector of the Gavião Block suggest the existence of an important event of crustal recycling, which in the Caraguataí suite originated magmatism related to a continental intraplate setting.

References

Alkmin, F.F., Brito Neves, B.B., Castro Alves, J.A., 1993. Arcabouço tectônico do Cráton do São Francisco: uma revisão. In: O Cráton do São Francisco. Dominguez, J.M.L. & Misi, A. (Eds.), SBG - Núcleo BA/SE, 45–62.

Arcanjo, J.B., Marques-Martins, A.A., Loureiro, H.S.C., Varela, P.H.L., 2000. Projeto vale do Paramirim, escala 1:100.000. Programa de Levantamentos Geológicos Básicos do Brasil. CD-ROM.

Babinski, M., Pedreira, A., Brito-Neves, B.B., Van-Schmus, W.R., 1999. Contribuição à geocronologia da Chapada Diamantina. In: SBG, Simpósio Nacional de Estudos Tectônicos, vol. 7, Anais, pp. 118–121.

Barbosa, J.S.F., Dominguez, J.M.L. (Eds.), 1996. Mapa Geológico do Estado da Bahia. Escala: 1.000.000. Texto explicativo, Salvador 382p.

Barbosa, J.S.F., Sabaté, P., 2002. Geological feature and the paleoproterozoic of four archean crustal segments of the São Francisco Craton, Bahia, Brazil. A synthesis. Anais da Academia Brasileira de Ciências 2, 343–359.

Barbosa, J.S.F., Sabaté, P., Leite, C.M.M., 2001. Os quatro blocos arqueanos do embasamento do Cráton do São Francisco na Bahia e a colisão no paleo-proterozóico. In: SBG/NNE, Simpósio Nacional de Estudos Tectônicos, vol. 8, Anais, pp. 131–133.

Bastos Leal, L.R.B., Cunha, J.C., Cordani, U.G., Teixeira, W., Nutman, A.P., Leal, A.B.M., Macambira, M.J.B., 2003. SHRIMP U–Pb, $^{207}Pb/^{206}Pb$ zircon dating, and Nd isotopic signature of the Umburanas Greenstone Belt, northern São Francisco Craton, Brazil. Journal of South American Earth Sciences 15, 775–785.

Bastos Leal, L.R.B., Teixeira, W., Cunha, J.C., Leal, A.B.M., Macambira, M.J.B., Rosa, M.L.S., 2000. Isotopic signatures of paleoproterozoic granitoids of the Gavião block and implications for the evolution of the São Francisco craton, Bahia, Brazil. Revista Brasileira de Geociências 30, 66–69.

Bastos Leal, L.R., 1998. Geocronologia U/Pb (SHRIMP), $^{207}Pb/^{206}Pb$, Rb–Sr, Sm–Nd e K–Ar dos Terrenos Granito-Greenstone do Bloco do Gavião: Implicações para Evolução arqueana e proterozóica do Cráton do São Francisco, Brasil. Tese de Doutoramento, Instituto de Geociências, Universidade Estado de São Paulo, 178p.

Bastos Leal, L.R., Teixeira, W., Cunha, J.C., Macambira, M.J.B., 1997. Crustal evolution of Gavião block of the São Francisco Craton: a geochronological study with, Pb–Pb, Sm–Nd, Rb–Sr and K–Ar. In: South American Symposium on Isotope Geology, 2, Extended Abstract, pp. 161–162.

Bastos Leal, L.R., Teixeira, W., Cunha, J.C., Macambira, M.J.B., 1998. Archean tonalitic–trondhjemitic and granitic plutonism in the Gavião block, São Francisco Craton, Bahia, Brazil: geochemical and geochronology characteristics. Revista Brasileira de Geociências 2, 209–220.

Bastos Leal, L.R., Teixeira, W., Macambira, M.J.B., Cordani, U., Cunha, J.C., 1996. Evolução crustal dos terrenos TTGs arqueanos do Bloco do Gavião, Cráton do São Franscisco: Geocronologia (SHRIMP) e Pb-Pb em zircões. In: SBG, Congresso Brasileiro de Geologia, vol. 39, Anais, pp. 539–541.

Best, M.G., 2003. Igneous and Metamorphic Petrology, second ed. Blackwell Publishing, 729 p.

Boynton, W.R., 1984. Cosmochemistry of the rare earth elements meteorite studies. In: Henderson, P. (Ed.), Rare Earth Element Geochemistry, pp. 63–114. Amsterdam.

Brito-Neves, B.B., Cordani, U.G., Torquato, J.R., 1980. Evolução geocronológica do Precambriano no estado da Bahia. In: Inda, H.A.D., Duarte, F.B. (Eds.), Geologia e Recursos Minerais do Estado da Bahia, vol. 3. SME-COM, pp. 1–101.

Buhn, B., Pimentel, M.M., Matteini, M., Dantas, E.L., 2009. High spatial resolution analysis of Pb and U isotopes for geochronology by laser ablation multicollector inductively coupled plasma mass spectrometry (LA-MC-ICP-MS). Anais da Academia Brasileira de Ciências 81, 1–16.

Collins, W.J., Beams, S.D., White, A.J.R., Chappell, B.W., 1982. Nature and origin of A-type granites with particular reference to Southeastern Australia. Contributions to Mineralogy and Petrology 80, 189–200.

Condie, K.C., Allen, P., 1984. Origin of Archaean charnokites from southern India. In: Kroner, A., et al. (Eds.), Archaean Geochemistry. Springer-Verlag, pp. 182–203.

Cordani, U.G., Iyer, S.S., 1979. Geochronological investigation on the Precambrian granulitic terrain of Bahia, Brazil. Precambrian Research 9, 255–257.

Cordani, U.G., Iyer, S.S., Taylor, P.N., Kawashita, K., Sato, K., Mcreath, I., 1992. Pb–Pb, Rb–Sr, and K–Ar systematics of the Lagoa Real uranium province (south-central Bahia, Brazil) and the Espinhaço Cycle (ca. 1.5–1.0 Ga). Journal of South American Earth Sciences 1, 33–46.

Cordani, U.G., Sato, K., Coutinho, J.M., Nutman, A., 1997. Geochronological interpretation in areas with complex evolution: the case of Piripá, central-southern Bahia, Brazil. In: South American Symposium on Isotope Geology, Extended Abstracts, pp. 85–87.

Cordani, U.G., Sato, K., Marinho, M.M., 1985. The geologic evolution of the ancient granite–greenstone terrane of central-southern Bahia, Brazil. Precambrian Research 27, 187–213.

Costa, P.H.O., Andrade, A.R.F., Lopes, G.A.C., Souza, S.L., 1985. Projeto Lagoa Real – Mapeamento Geológico 1:25.000, vol. 1. CBPM/NUCLEBRAS/SME. 455p.

Creaser, R.A., Price, R.C., Wormald, R.J., 1991. A-type granites: assessment of a residual-source model. Geology 19, 163–166.

Cruz, S.C.P., 2004. A interação tectônica entre o Aulacógeno do Paramirim e o Orógeno Araçuaí-Oeste Congo. Tese de Doutorado, Departamento de Geologia, UFOP, 505 p.

Cruz, S.C.P., Alkmim, F.F., Leite, C.M.M., Evangelista, H.J., Cunha, J.C., Matos, E.C., Noce, C.M., Marinho, M.M., 2007. Geologia e arcabouço estrutural do Complexo lagoa Real, Vale do Paramirim, Centro-Oeste da Bahia. Revista Brasileira de Geociências 4 (suplemento), 28–146.

Cunha, J.C., Leal, L.R., Fróes, R.J.B., Teixeira, W., Macambira, M.J.B., 1996. Idade dos greenstone belts e dos terrenos TTG's associados da região de Brumado, centro oeste do Cráton do São Francisco (Bahia-Brasil). In: SBG, Congresso Brasileiro de Geologia, vol. 39, Anais, pp. 67–70.

Danderfer Filho, A., Dardenne, M.A., 2002. Tectonoestratigrafia da Bacia Espinhaço na porção centro-norte do Cráton do São Francisco: registro de uma evolução polihistórica descontínua. Revista Brasileira de Geociências 4, 449–460.

Danderfer Filho, A., 1990. Análise estrutural descritiva e cinemática do Supergrupo Espinhaço na região da Chapada Diamantina (BA). Dissertação de Mestrado, Departamento de Geologia, Universidade Federal de Ouro Preto, 99p.

Danderfer Filho, A., 2000. Geologia sedimentar e evolução tectônica do Espinhaço Setentrional, estado da Bahia. Tese de Doutorado, Instituto de Geociências, Universidade Federal de Brasília, 497p.

Danderfer Filho, A., DeWaele, B., Pedreira, A., Nalini, H.A., 2009. New geochronological constraints on the geological evolution of the Espinhaço basin within the São Francisco Craton—Brazil. Precambrian Research 170, 116–128.

De La Roche, H., Leterrier, J., Grandcloude, P., Marchal, M., 1980. A classification of volcanic and plutonic rocks using R1R2 diagram major-elements analyses its relationships with current nomenclature. Chemical Geology 29, 183–210.

DePaolo, D.J., 1988. Neodymium Isotope Geochemistry, an Introduction. Springer-Verlag, Berlin, 187 p.

Duchesne, J.C., Wilmart, E., 1997. Igneous charnockites and related rocks from the Bjerkreim-Sokndal layered intrusion (Southwest Norway): a jotunite (hypersthene monzodiorite)-derived A-type granitoid suite. Journal of Petrology 38, 337–369.

Eby, G.N., 1992. Chemical subdivision of the A-type granitoids: petrogenetic and tectonic implications. Geology 20, 641–644.

Eby, G.N., 1990. The A-type granitoids: a review of their occurrence and chemical characteristics and speculations on their petrogenesis. Lithos 26, 115–134.

Emslie, R.F., 1991. Granitoids of rapakivi granite–anorthosite and related associations. Precambrian Research 51, 173–192.

Fernandes, P.E.C.A., Montes, M.L., Braz, E.R.C., Silva, L.L., Oliveira, F.L.L., Ghignone, J.I., Siga Jr., O., Castro, H.E.F., 1982. Geologia. In: BRASIL. Ministério das Minas e Energia. Secretaria Geral. Projeto RADAMBRASIL. Folha SD.23 Brasília: geologia, geomorfologia, pedologia, vegetação e uso potencial da terra. Rio de Janeiro, pp. 25–204.

Frost, B.J., Barnes, C.J., Collins, W.J., Arculus, R.J., Ellis, D.J., Frost, C.D., 2001. A geochemical classification for Granitic Rocks. Journal of Petrology 42, 2033–2048.

Gioia, S.M., Pimentel, M.M., 2000. The Sm–Nd isotopic method in the geochronology laboratory of the University of Brasília. Anais da Academia Brasileira de Ciências 2, 219–245.

Guimarães, J.T., Teixeira, L.R., Silva, M.G., Martins, A.A.M., Filho, E.L.A., Loureiro, H.S.C., Arcanjo, J.B., Dalton de Souza, J., Neves, J.P., Mascarenhas, J.F., Melo, R.C., Bento, R.V., 2005. Datações U/Pb em rochas magmáticas intrusivas no Complexo Paramirim e no Rifte Espinhaço: Uma contribuição ao estudo da Evolução Geocronológica da Chapada Diamantina. In: SBG/BA-SE, Simpósio do Cráton do São Francisco, Salvador, Anais de Resumos Expandidos, pp. 159–161.

Guimarães, J.T., 1996. A Formação Bebedouro no Estado da Bahia: Faciologia, Estratigrafia e Ambiente de Sedimentação. Dissertação de Mestrado, Instituto de Geociências, Universidade Federal da Bahia, 155p.

Irvine, T.N., Baragar, V.R.A., 1971. A guide to the chemical classification of common volcanic rocks. Canadian Journal of Earth Sciences 8, 523–548.

Jahn, B.M., Zhang, Z.Q., 1984. Radiometric ages (Rb–Sr, Sm–Nd, U–Pb) and REE geochemistry of Archaean grunulite gneisses from Eastern Hebei Province. China. In: Kroner, A., et al. (Eds.), Archaean Geochemistry. Springer-Verlag, pp. 204–234.

Jardim de Sá, E.F., 1981. A Chapada Diamantina e a faixa Santo Onofre: Um exemplo de tectônica intraplaca no Proterozóico Médio do Cráton São Francisco. In: Inda, H.A.A.V., Marinho, M.M., Duarte, F.B. (Eds.), Geologia e Recursos Minerais do Estado da Bahia, Textos Básicos, vol. 4. SME/COM, pp. 111–120.

Ledru, P., Cocherie, A., Barbosa, J.S.F., Johan, V., Onstott, T., 1993. Âge du Métamorphisme granulitique dans Le Craton Du São Francisco (Brésil): Inplications Sur la nature de lórogene transmazoneen. Comptes Rendus de l'Académie des Sciences, Paris 211, 120–125.

Liégeois, J.P., Navez, J., Hertogen, J., Black, R., 1998. Contrasting origin of postcollisional high-K calc-alkaline and shoshonitic versus alkaline and peralkaline granitoids. Lithos 45, 1–28.

Lobato, L.M., 1985. Metamorphism, metasomatism and mineralization at Lagoa Real, Bahia, Brazil. Tese de Doutoramento, University Western Ontario, 306p.

Lobato, L., Fyfe, W., 1990. Metamorphism and mineralization at Lagoa Real, Bahia, Basil. Economic Geology 5, 968–989.

Lopes, G.A.C., 1991. In: Investigação da metalogênese de granitóides da região de Vitória da Conquista, vol. 1. SME/CBPM textos e mapas. 70p.

Lopes, G.A.C., 2002. Projeto Guajeru, vol. 1. CBPM, Salvador. 408p.

Loureiro, H.S.C., Lima, E.S., Macedo, E.P., Silveira, F.V., Bahiense, I.C., Arcanjo, J.B.A., Moraes-Filho, J.C., Neves, J.P., Guimarães, J.T., Rodrigues, L.T., Abram, M.B., Santos, R.A., Melo, R.C., 2010. Geologia e Recursos Mineris da Parte norte do Corredor de Deformação do Paramirim: Projeto Barra-Oliveira dos Brejinhos. CBPM, Salvador. 118p. il. Série Arquivos Abertos, 33.

Ludwig, K.R., 2003. Isoplot/EX, version 3. A Geochronological Toolkit for Microsoft Excel. Berkeley Geochronology Center, Special Publication, 4, 70 p.

Marinho, M.M., 1991. La séquence volcano-sédimentaire de Contendas Mirante et la bordure occidentale du Bloc de Jéquié (Craton du São Francisco, Brésil): un exemple de transition Archéan-Protérozoique. Thèse de l'Université de Clemont-Ferrand, 257p.

Marinho, M.M., Rios, D.C., Conceição, H., Rosa, M.L.S., 2008. Magmatismo alcalino neoarqueano no Cráton do São Francisco, Bahia: pluton Pé de Serra. In: SBG, Congresso Brasileiro de Geologia, vol. 44, Anais, p. 57.

Marinho, M.M., Costa, P.H., Silva, E.F.A., Torquato, J.R., 1979. Evolução Geotectônica do Pré-cambriano no Estado da Bahia. In: Inda, H.A.V. (Ed.), Geologia e recursos minerais do Estado da Bahia, textos básicos. SME/CPM, Salvador, pp. 57–157.

Martin, H., Peucat, J.J., Sabaté, P., Cunha, J.C., 1991. Um segment de croûte continentale d'Age archéean ancien (3.5 millards d'années): lê massif de Sete Voltas (Bahia, Brésil). Comptes Rendus de l'Académie des Sciences, Paris 313, 531–538.

Martin, H., Smithies, R.H., Rapp, R., Moyen, J.F., Champion, D., 2005. An overview of adakite, tonalite–trondhjemite–granodiorite (TTG) and sanukitoid: relationships and some implications for crustal evolution. Lithos 79, 1–24.

Martin, H., Peucat, J.J., Sabaté, P., Cunha, J.C., 1997. Crustal evolution in the early Archaean of South America: example of the Sete Voltas Massif, Bahia State, Brazil. Precambrian Research 82, 35–62.

Mascarenhas, J.F., Garcia, T.M., 1989. Mapa geocronológico do estado da Bahia. Secretaria de Minas e Energia, Texto Explicativo, Salvador, Bahia. 130p.

McReath, I., Sabaté, P., 1987. Granitoids of the Bahia State, Brazil: a review. Revista Brasileira de Geociências 4, 404–414.

Misi, A., Veizer, J., 1996. Chemostratigraphy of neoproterozoic carbonate sequences of the Una Group, Irecê Basin, Brazil. In: SBG/NBA-SE, Congresso Brasileiro de Geologia, 39, Anais, vol. 5, pp. 487–489.

Noce, C.M., Pedrosa-Soares, A.C., Silva, L.C., Armstrong, R., Piuzana, D., 2007. Evolution of polycyclic basement complexes in the Aracuaí Orogen, based on U–Pb SHRIMP data: implications for Brazil–Africa links in Paleoproterozoic time. Precambrian Research 159, 60–78.

Nutman, A.P., Cordani, U.G., 1993. SHRIMP U–Pb zircon geochronology of Archean granitoids from the Contendas Mirante area of the São Francisco Craton, Bahia, Brazil. Journal of South American Earth Sciences 7, 107–114.

Nutman, A.P., Cordani, U.G., Sabaté, P., 1993. SHRIMP ages of detrital zircons from the early Proterozóic Contendas-Mirante supracrustal belt, São Francisco Craton, Bahia, Brazil. Journal of South American Earth Sciences 7, 109–114.

Oliveira, E.P., Mello, E.F., McNaughton, N., 2002. Reconnaissance U–Pb geochronology of Precambrian quartzites from the Caldeirão belt and their basement, NE São Francisco Craton, Bahia, Brazil: implications for the early evolution of the Paleoproterozoic ITab una–Salvador–Curacá Orogen. Journal of South American Earth Sciences 15, 349–362.

Oliveira, E.P., Souza, Z.S., Corrêa-Gomes, L.C., 2000. U–Pb dating of deformed mafic dyke and host gneiss: implications for understanding reworking processes on the western margin of the archaean Uaua Block, NE São Francisco Craton, Brazil. Revista Brasileira de Geociências 1, 149–152.

Patiño Douce, A.E., 1997. Generation of metaluminous A-type granites by low-pressure melting of calc-alkaline granitoids. Geology 25, 743–746.

Pearce, J.A., 1996. Sources and settings of granitic rocks. Episodes 19, 120–125.

Pedrosa-Soares, A.C., Noce, C.M., Alkmim, F.F., Silva, L.C., Babinski, M., Cordani, U., Castañeda, C., 2007. Orógeno Araçuaí: síntese do conhecimento 30 anos após Almeida 1977. Geonomos 1, 1–16.

Peucat, J.J., Mascarenhas, J.F., Barbosa, J.S.F., de Souza, S.L., Marinho, M.M., Fanning, C.M., Leite, C.M.M., 2002. 3.3 Ga SHRIMP U–Pb zircon age of a felsic metavolcanic rock from the Mundo Novo Greenstone belt in the São Francisco Craton, Bahia (NE Brazil). South American Journal of Earth Sciences 15, 363–373.

Pimentel, M.M., Machado, N., Lobato, L.M., 1994. Geocronologia U/Pb de rochas graníticas e gnáissicas da região de Lagoa Real, Bahia, e implicações para a idade da mineralização de urânio. In: SBG, Congresso Brasileiro de Geologia, vol. 38, Boletim de Resumos Expandidos, pp. 389–390.

Pupin, J.P., 1980. Zircon and granite petrology. Contributions to Mineralogy and Petrology 73, 207–220.

Rosa, A.M.L.S., Conceição, H., Paim, M.M., Santos, E.B., Alves, F.C., Leahy, G.S., Leal, L.R., 1996. Magmatismo potássico/ultrapotássico Pós a tardi orogênico associado à subducção no oeste da Bahia: Batólito Monso-sienitico de Guanambi-Urandi e os sienitos de Correntina. Geochimica Brasiliensis 1, 027–042.

Sabaté, P., Marinho, M.M., Vidal, P., Vauchette, M., 1990. The 2-Ga peraluminous magmatism of the Jacobina-Contendas-Mirante Belts (Bahia, Brazil): geologic and isotopic constraints on the sources. Chemical Geology 83, 325–338.

Santos-Pinto, M.A.S., Peucat, J.J., Martin, H., Sabaté, P., 1998. Recycling of the Archaean continental crust: the case study of the Gavião Block, Bahia, Brazil. Journal of South American Earth Sciences 11, 487–498.

Santos-Pinto, M.A., 1996. Le recyclage de la croûte continentale archéenne: Exemple du bloc du Gavião-Bahia, Brésil. Mémoire de Géociences Rennes 75 193p.

Santos-Pinto M., Peucat J.J., Martin H., Barbosa J.S.F., Fanning C.M., Cocherie A., Paquette J.L., Submitted for publication. Crustal evolution between 2.0 and 3.5 Ga in the southern Gavião block (Umburanas-Brumado-Aracatu region), São Francisco Craton, Brazil. A 3.5-3.8 Ga proto-crust in the Gavião block? Jour of South America Earth Sciences.

Sato, K., 1998. Evolução crustal da plataforma sul americana, com base na geoquímica Isotópica SM-Nd. Tese de Doutorado, Instituto de Geociências, Universidade de São Paulo, 297p.

Schobbenhaus, C., 1996. As tafrogêneses superpostas Espinhaço e Santo Onofre, estado da Bahia: Revisão e novas propostas. Revista Brasileira de Geociências 4, 265–276.

Schobbenhaus, C., Hoppe, A., Baumann, A., Lork, A., 1994. Idade U/Pb do vulcanismo Rio dos Remédios, Chapada Diamantina, Bahia. In: SBG, Congresso Brasileiro de Geologia, 38, Anais, vol. 2, pp. 397–399.

Silva, M.G., Cunha, J.C., 1999. Greenstone Belts and equivalent volcano-sedimentary sequences of the São Francisco Craton, Bahia, Brazil, Brazil – Geology and Mineral Potential. In: Silva, M.G., Misi, A. (Eds.), Base Metal deposits of Brazil. MME/CPRM/DNPM, Belo Horizonte, pp. 92–99.

Simpsom, C., 1985. Deformation of granitic rocks across the brittle–ductile transition. Journal of Structural Geology 7, 503–511.

Simpson, C., 1986. Fabric development in brittle-to-ductile shear zones. Pure and Applied Geophysics 124, 269–288.

Smith, D.R., Noblett, J., Wobus, R.A., Unruh, D., Douglass, J., Beane, R., Davis, C., Goldman, S., Kay, G., Gustavson, B., Saltoun, B., Stewart, J., 1999. Petrology and geochemistry of late-stage intrusions of the A-type, mid-Proterozoic Pikes Peak batholith (Central Colorado, USA): implications for petrogenetic models. Precambrian Research 98, 271–305.

Stipp, M., Stünitz, H., Heilbronner, R., Schmid, S.M., 2002. Dynamic recrystallization of quartz: correlation between natural and experimental conditions. In: De Meer, S., Drury, M.R., De Bresser, J.H.P., Pennock, G.M. (Eds.), Deformation Mechanisms, Rheology and Tectonics: Current Status and Future Perspectives. Geological Society, London, Special Publications, 200, pp. 171–190.

Teixeira, L.R., 2000. Projeto Vale do Paramirim. Relatório Temático de Litogeoquímica. Convênio CPRM/CBPM.

Teixeira, W., Carneiro, M.A., Noce, C.M., Machado, N., Sato, K., Taylor, P.N., 1996. Pb, Sr and Nd isotope constraints on the Archaean evolution of gneissic–granitoid complexes in the southern São Francisco Craton, Brazil. Precambrian Research 78, 151–164.

Teixeira, W., Cordani, U.G., Nutman, A.P., Sato, K., 1998. Polyphase Archean evolution in the Campo Belo metamorphic complex, Southern SaÄ o Francisco Craton, Brazil: SHRIMP U–Pb zircon evidence. Journal of South American Earth Sciences 3, 279–289.

Tullis, J., 1983. Deformation of feldspar. In: Ribbe, P.H. (Ed.), Feldspar Mineralogy, vol. 2. Mineralogical Society of America, Washington, pp. 297–323.

Turpin, L., Maruèjol, P., Cuney, M., 1988. U–Pb, Rb–Sr and Sm–Nd chronology of granitic basement, hydrothermal albitites and uranium mineralization, Lagoa Real, South Bahia, Brazil. Contribution to Mineralogy and Petrology 98, 139–147.

Vauchez, A., 1987. The development of discrete shear-zones in a granite: stress, strain and changes in deformation mechanisms. Tectonophysics 133, 137–156.

Waever, L.W., Tarney, J., 1980. Rare earth geochemistry of Lewisian granulite-facies gneisses, Northwest Scotland: implications for the petrogenesis of the Archaean lower continental crust. Earth and Planetary Science Letters 51, 279–296.

Whalen, J.B., Currie, K.L., Chappell, B.W., 1987. A-type granites: geochemical characteristics, discrimination and petrogenesis. Contribution to Mineralogy and Petrology 95, 407–419.

Wilson, N., Moorbath, S., Taylor, P.N., Barbosa, J., 1988. Archean and early Proterozoic crustal evolution in the São Francisco Craton, Bahia, Brazil. Chemical Geology 70, 47.

Wood, D.A., Joron, J.L., Treuil, M., Norry, M., Tarney, J., 1979. Elemental and Sr isotope variations in basic lavas from Iceland and the surrounding ocean floor. Contribution to Mineralogy and Petrology 70, 319–339.